DEPARTMENT OF COMMERCE
LUTHER H. HODGES, Secretary

WEATHER BUREAU
F. W. REICHELDERFER, Chief

MONTHLY WEATHER REVIEW

JAMES E. CASKEY, JR., Editor

Volume 89, Number 10 | Washington, D.C. | October 1961

CLOUD STREETS OVER THE CARIBBEAN SEA[1]

JOHN SCHUETZ AND SIGMUND FRITZ

U.S. Weather Bureau, Washington, D.C.

[Manuscript received June 23, 1961]

ABSTRACT

Bands of cumuliform clouds over the Caribbean Sea as observed by TIROS I are described. The possible relationship between the occurrence of these bands and the vertical structure of the horizontal winds is discussed. The cloud street orientation is compared with the wind direction.

1. INTRODUCTION

The meteorological satellite, TIROS I, [1] presented an opportunity to view the meso-scale structure of cloud systems as well as the large-scale structure [2, 3, 4, 5]. The meso-scale structure is often better shown by the "narrow angle" camera. This camera when pointing vertically downward from a height of 380 n. mi., photographed an area whose diagonal was about 85 miles across. This detail enables one to study several interesting features of "cloud streets."

Such long thin lines of clouds, or cloud streets, occur fairly frequently in the atmosphere. For example, Riehl et al. [6], in a study of cumulus cloud bands in the tropical Pacific, found that the bands were oriented parallel to the low-level wind flow. Kuettner [7] presented several examples in which cumulus cloud streets were parallel to the wind; he also discussed the meteorological conditions under which such cloud bands will align with the wind. He considered mainly cloud streets formed when cold air flows over warm surfaces, although other types were also mentioned.

The TIROS I narrow angle camera also photographed some cumulus cloud streets, and the relationship of the flow patterns to the orientation and other aspects of the streets shown in the pictures will be discussed below.

[1] This research has been supported by the National Aeronautics and Space Administration.

2. THE SATELLITE PICTURES

Figure 1 is a composite assembled from several narrow-angle pictures taken at 10-second intervals between 2030 GMT and 2033 GMT on April 1, 1960. The satellite was traveling from northwest to southeast which is from left to right in the composite. The camera axis was oriented slightly back and to the left at this time.

The white areas in figure 1 are probably all cumuliform clouds. Grand Cayman Island is relatively cloud-free while the western end of Cuba and the Isle of Pines are more cloud covered. The presence of such land features increases the confidence in the location and orientation of the cloud features.

Figure 2 is a schematic representation of the clouds shown in figure 1. The dashed outline defines the areal coverage of figure 1. The track of the satellite is shown by the arrow.

The composite and the schematic diagram indicate a greater concentration of cumulus clouds over the heated land areas of the Isle of Pines and Cuba than over the adjacent ocean areas. This is perhaps better shown by examining figures 3 and 4 which depict the detail of cloud masses over Cuba and over the Isle of Pines, respectively. (The shoreline of the islands is indicated by the white outline.) These figures show much more extensive cumulus activity over the heated islands than over the adjacent ocean areas.

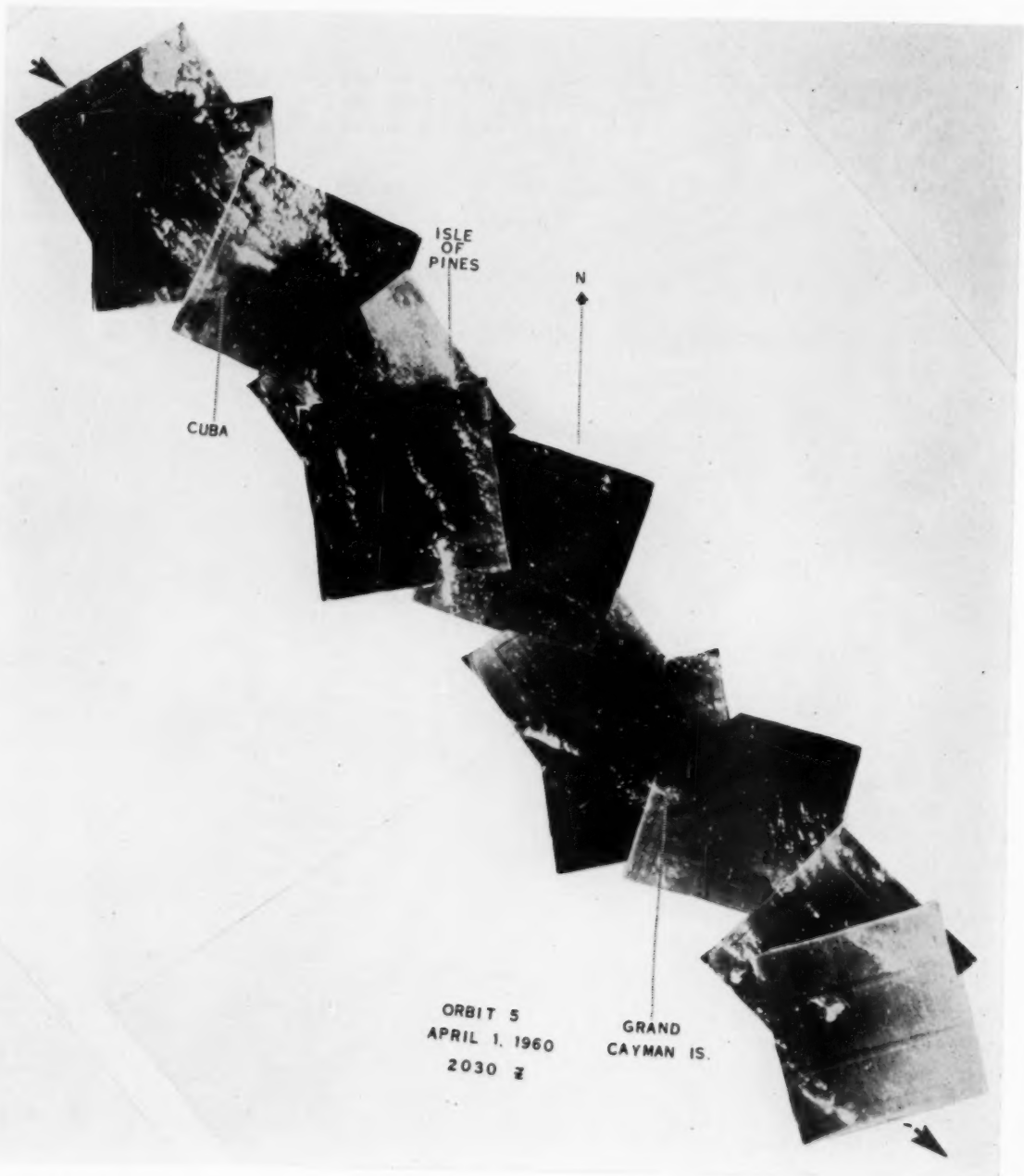

FIGURE 1.—Mosaic of narrow-angle pictures taken at 10-sec. intervals between 2030 and 2033 GMT, April 1, 1960.

This more extensive convective activity is apparently indicative of the greater instability over the islands. In figure 5, comparison of the 0000 GMT, April 2, 1960 radiosonde observations at Havana (considered representative of the heated air over the island of Cuba) with the radiosonde at Grand Cayman (considered representative of the oceanic air) shows the Grand Cayman sounding to be more stable and drier, particularly in the layer from 900 to 800 mb. Differences in heating doubtlessly account for much of this stability difference. An inspection of the sounding for 0000 GMT, April 2 and for 12 hours earlier (not shown here) at Havana (land influence) and at Grand Cayman (oceanic influence) shows that the lower layer at Havana experienced considerably more warming between early morning and evening than did the lower layer at Grand Cayman.

3. CLOUD STREETS IN RELATION TO THE WIND FIELD

The tendency for cumulus clouds to line up in bands or streets under certain conditions has been pointed out [6, 7]. Kuettner [7] discusses some conditions required for the convectively formed clouds to align in bands parallel to the wind. In his observation, the wind direction was fairly constant throughout the convective layer; but a wind-speed maximum also existed within the convective layer giving a negative mean curvature. The important parameter, according to Kuettner [7], in determining whether such bands will align with the wind is the mean curvature of the vertical profile of the horizontal wind speed within the convective layer. He found typical values of this speed-curvature to be of the order of -10^{-7} cm.$^{-1}$ sec.$^{-1}$

Figure 6 shows the wind direction and speed at Havana and at Grand Cayman as a function of height. (Note: The 0000 GMT April 2 wind record for Havana was missing; therefore the 1200 GMT April 1 wind sounding was used. This difference is probably not serious since the synoptic situation in this region was generally unchanged in this 12-hour period.) The Grand Cayman wind profile (fig. 6b) shows a well defined, broad wind speed maximum in the lower layers while Havana (fig. 6a) shows a poorly defined slight maximum at 10,000 feet. Although the wind maximum may not be significant for Havana, computation of the mean curvature in the first 12,000 feet indicated that at both stations the wind profile curvatures were negative, and the curvature had values within an order of magnitude of 10^{-7} cm.$^{-1}$ sec.$^{-1}$

The cloud mosaic (fig. 1) and cloud schematic (fig. 2) show the cloud bands in the vicinity of the Isle of Pines and Cuba oriented at about 140°, and the three cloud bands just southeast of the Isle of Pines oriented at 150°–160°. Referring to figure 6a, it can be seen that the winds at Havana in the first 12,000 feet were within 30° of these orientations. In the layer from 2,000 to 12,000 feet, the wind at Grand Cayman was between 120° and 140°. Thus the cloud streets are aligned quite closely with the wind direction in the convective layer at the two stations.

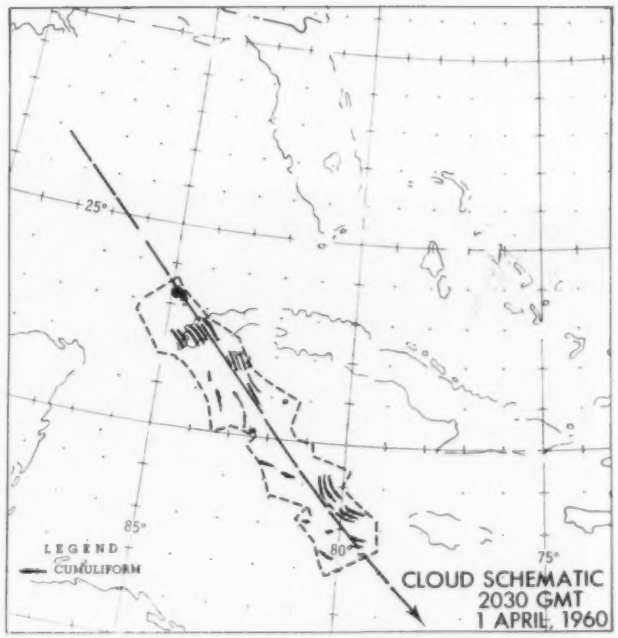

FIGURE 2.—Map showing schematic representations of cloud features appearing on the mosaic of figure 1. The irregular outline delineates geographic coverage of the mosaic. The track of the satellite is indicated by the arrow.

Satellite pictures present an opportunity to observe spacing, shape, and other characteristics of cloud bands. For example, the three cloud bands immediately south and southeast of the Isle of Pines just mentioned (see fig. 1) are interesting because of their length and of the large distances between them. Figure 7 shows these three bands in greater detail. The distance from the easternmost band in figure 7 to the middle one is about 20 miles, and from the middle band to the westernmost one is about 30 miles. The length of the middle band (neglecting the brighter portion in the south which may be part of another cloud band) is about 30 miles, and of the other two about 50 miles.

Noting again figures 3 and 4, one can see that over the heated land masses of the Isle of Pines and Cuba the spacing of the bands is an order of magnitude smaller than the spacing over the ocean. Over Cuba the spacing is about 3 to 4 miles; over the Isle of Pines it is about 2 to 3 miles. Moreover, the length of these lines appears to be related to the distance across the island in the direction of the wind flow. For example, the bands (fig. 3) over extreme western Cuba are shorter than those farther east over Cuba; the bands over the very narrow southwestern portion of the Isle of Pines (fig. 4) are much

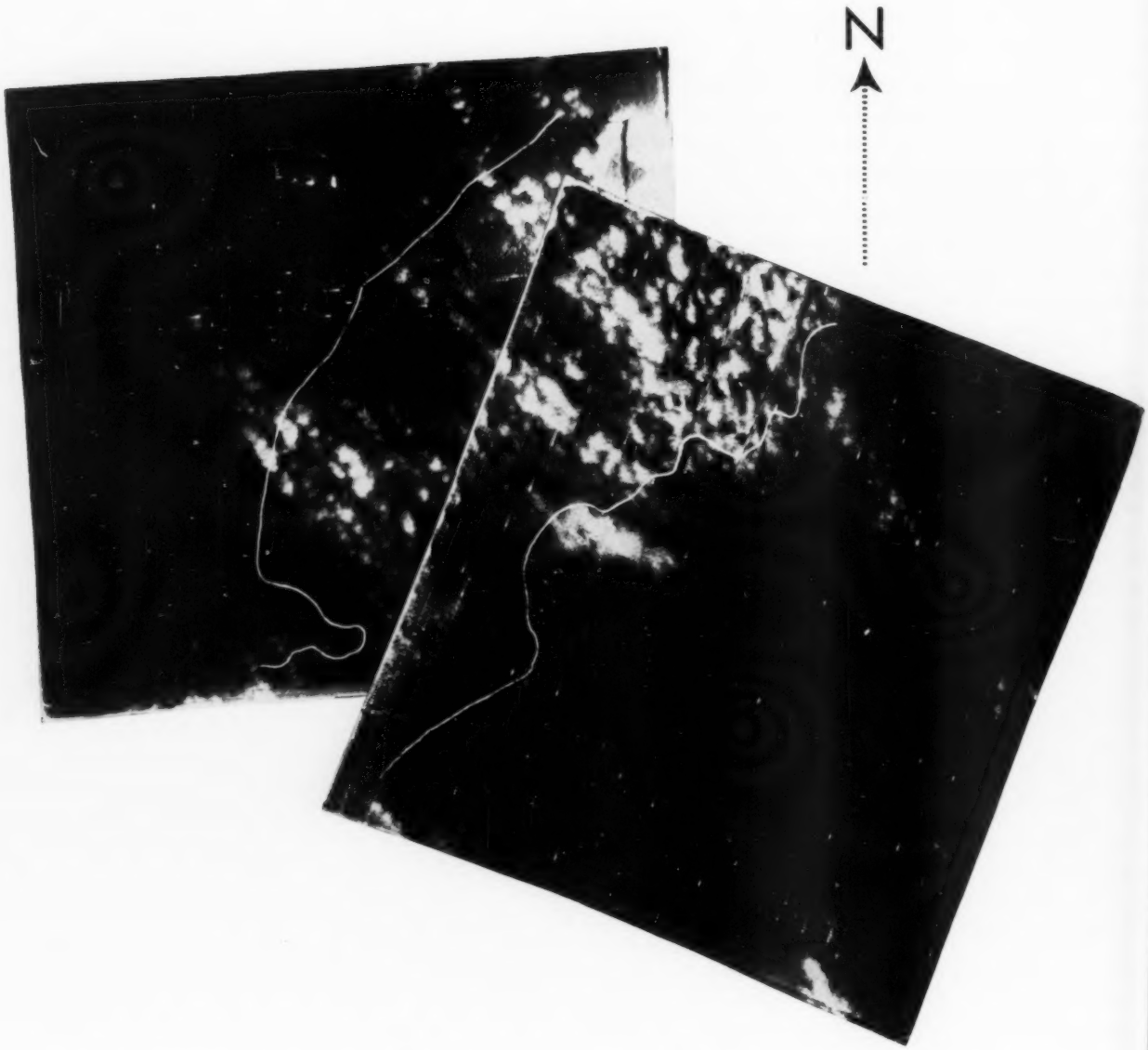

FIGURE 3.—Detailed composite of the portion of the mosaic over Cuba. The Cuban coastline is shown by the white outline.

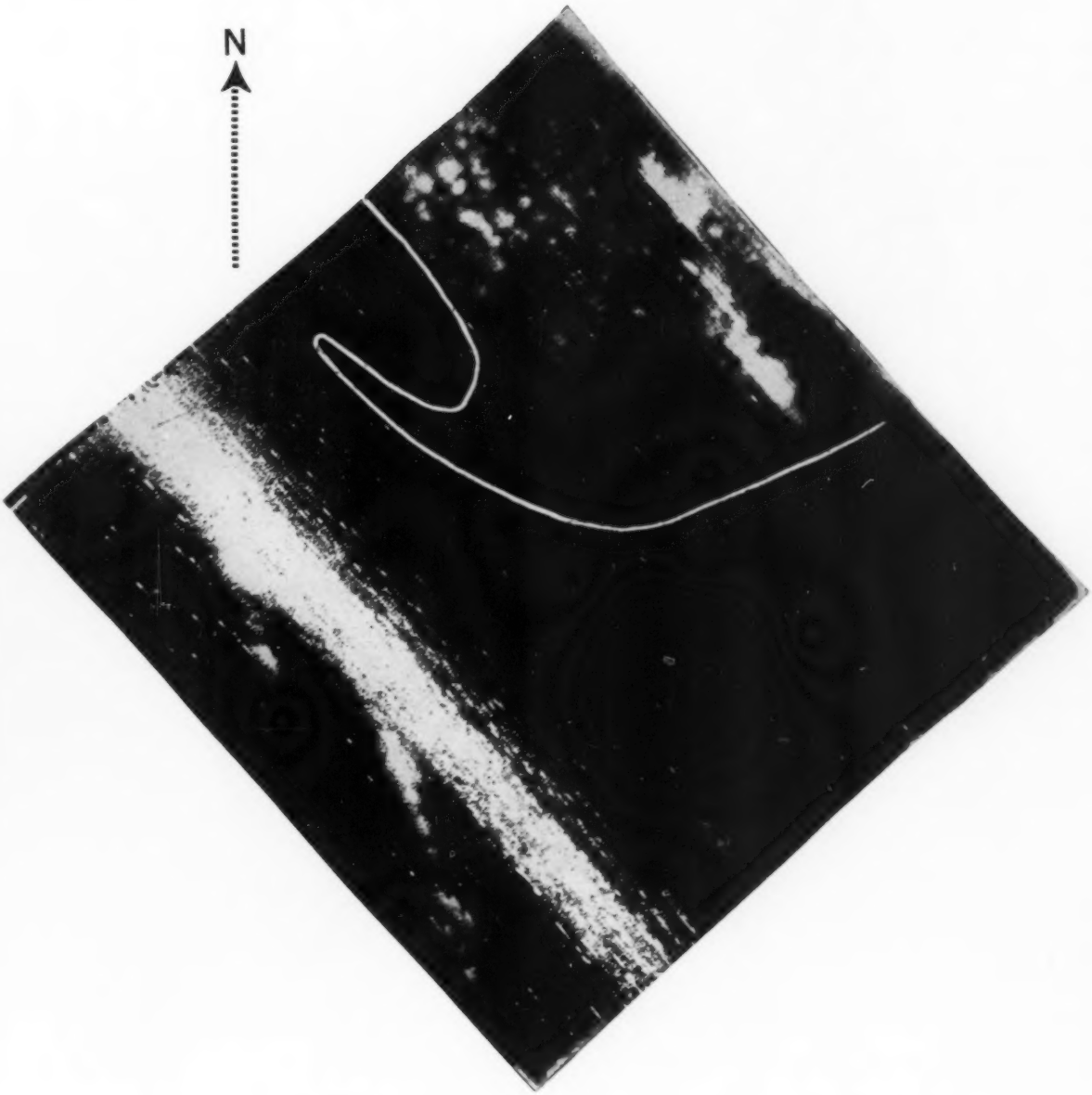

FIGURE 4.—Detailed view of cloud streets over the Isle of Pines. The coastline is depicted by the white outline.

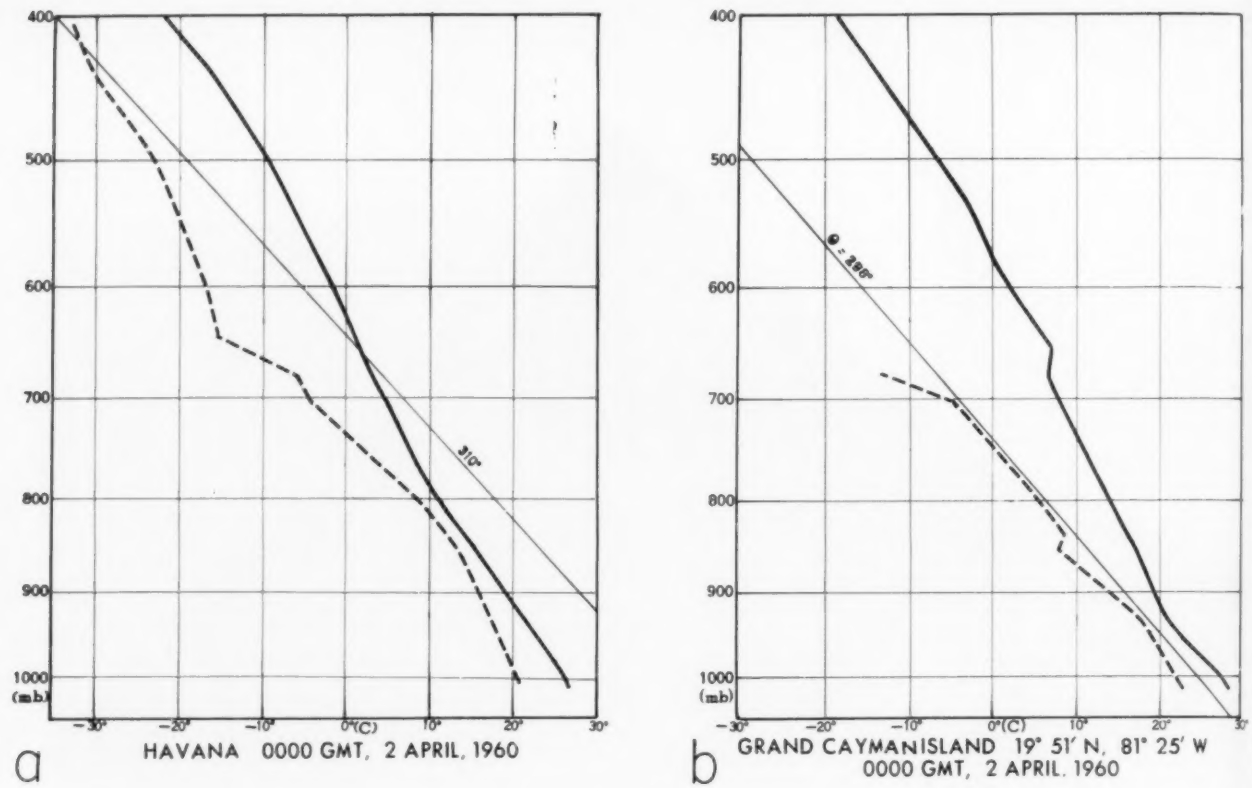

FIGURE 5.—Radiosonde observations for Havana and Grand Cayman Island at 0000 GMT, April 2, 1960.

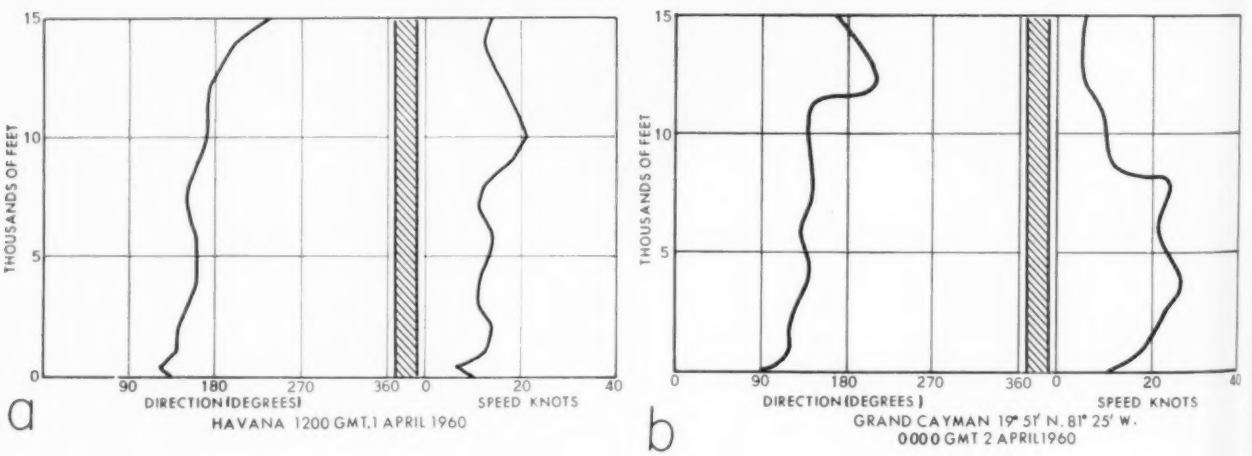

FIGURE 6.—Graph of wind speed and direction as a function of height for Havana at 1200 GMT, April 1, 1960 and Grand Cayman at 0000 GMT, April 2, 1960.

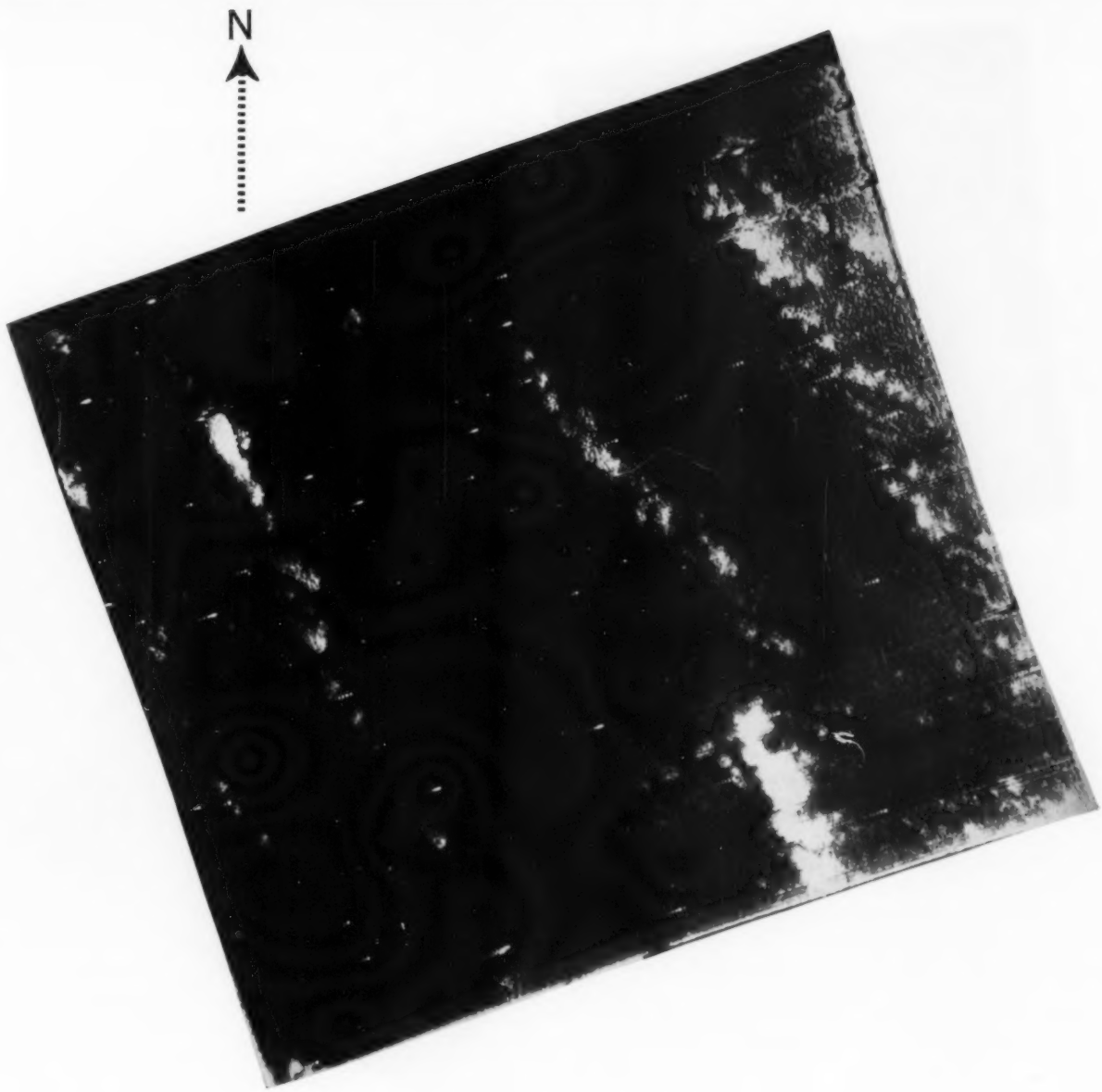

FIGURE 7.—Larger picture of the three oceanic cloud bands in figure 1.

shorter than those over the northeastern portion of the island. The distances across the islands in the direction of the wind flow vary in a similar manner.

In the extreme southeastern end of the picture swath, some anticyclonically (?) curved bands, which were imbedded in the general southeastern flow, were noted (see figs. 1 and 2). These are illustrated more clearly in figure 8. The radius of curvature of these bands is 60 n.mi. and they are spaced at 3 to 4-n.mi. intervals. Meteorological observations in this area were too sparse to determine whether a circulation of such a small scale existed. Nevertheless the curvature in the cloud street suggests that such small undulations in the circulation may have existed.

4. SUMMARY

The TIROS narrow-angle camera presents a means of determining such factors as orientation, spacing, and length of cloud streets. In this study the streets were aligned within 30° of the wind direction in the convective layer. The spacing of the streets over heated land was much less than of those over the ocean. The length of the streets over the larger islands appeared to be related to the distance across the island in the direction of the wind flow.

FIGURE 8.—Composite showing greater detail of the curved bands in figure 1.

REFERENCES

1. S. Sternberg et al., "Roundup on TIROS I," *Astronautics*, vol. 5, No. 6, June 1960.
2. S. Fritz and H. Wexler, "Cloud Pictures From Satellite TIROS I," *Monthly Weather Review*, vol. 88, No. 3, Mar. 1960, pp. 79–87.
3. J. S. Winston and L. Tourville, "Cloud Structure of an Occluded Cyclone Over the Gulf of Alaska as Viewed by TIROS I," *Bulletin of the American Meteorological Society*, vol. 42, No. 3, Mar. 1961, pp. 151–166.
4. S. Fritz, "Satellite Cloud Pictures of a Cyclone over the Atlantic Ocean," *Quarterly Journal of the Royal Meteorological Society*, vol. 87, No. 373, July 1961, pp. 314–321.
5. C. L. Bristor and M. A. Ruzecki, "TIROS I Photographs of the Midwest Storm of April 1, 1960," *Monthly Weather Review*, vol. 88, Nos. 9–12, Sept.–Dec. 1960, pp. 315–326.
6. H. Riehl, W. S. Gray, J. S. Malkus, and C. Ronne, "Cloud Structure and Distributions over the Tropical Pacific," Unpublished manuscript, Woods Hole Oceanographic Institution, 66 pp., 1959. Ref. No. 58–62, Technical Report No. 5, ONR Contract Number 1721(00).
7. J. Kuettner, "The Band Structure of the Atmosphere," *Tellus*, vol. 11, No. 3, Aug. 1959, pp. 267–294.

A WESTERN ATLANTIC VORTEX SEEN BY TIROS I

J. B. JONES, MAJOR, USAF

Air Weather Service Member, Meteorological Satellite Laboratory, U.S. Weather Bureau, Washington, D.C.

[Manuscript received April 14, 1961; revised June 29, 1961]

ABSTRACT

TIROS I observed an extratropical cyclone near Bermuda on three occasions in early May 1960 during the last 86 hours of the life cycle of the storm. A study of this case was undertaken with three objectives in mind: (a) to describe interesting features of the organization manifested in the cloud patterns and compare these with conventional analyses; (b) to present a subjective interpretation of some of the cloud images and discuss the criteria which form the basis for interpretation; and (c) to show examples of practical application of these pictures of the storm to routine frontal analysis and nephanalysis.

1. INTRODUCTION

During early May 1960, TIROS I took pictures of a small extratropical vortex located in the western Atlantic between Bermuda and the southeastern United States. Pictures were obtained during the mid-afternoon on May 5, 7, and 8. On May 6 the orbital passes over the region were too far east or west of the vortex for the satellite to view the associated cloud patterns. Included in this paper are a brief synoptic history of the storm, a description and subjective interpretation of the cloud images, a brief discussion of the apparent relation between the cloud patterns and conventional analyses, and finally a demonstration of the practical utility of the cloud pictures obtained by a satellite.

In recent months, storms observed by TIROS I over the eastern Pacific Ocean, the central United States, and the northeastern Atlantic Ocean have been studied [1, 7, 12, 15]. Some of these studies deal essentially with a single observation of the storm [1, 12]. In other cases successive views of the same system have permitted a study of persistent and transient features of the associated cloud patterns over time intervals varying from 100 minutes to approximately 24 hours [7, 15]. For the case presented in this paper, a fortuitous set of circumstances provided pictures of the same storm at 48- and 24-hour intervals over a 4-day period, recording on film the degeneration of a vigorous cyclone.

2. SYNOPTIC HISTORY

Indications of a wave formation on the polar front in the Atlantic immediately east of Florida appeared on the NAWAC surface analysis for 0000 GMT, May 3, 1960 (fig. 1a). During the next 72 hours, the wave continued to develop and apparently reached maximum intensity at about 0000 GMT, May 6 (figs. 1b-d). Subsequently the low center retrograded (figs. 1e-f), the associated frontal system became diffuse and ill defined, and finally during the period 0000 GMT to 1200 GMT May 9, the vortex filled and disappeared (figs. 1g-h).

3. THE PICTURES

ORGANIZATION

The storm was first viewed by TIROS on May 5 near 2200 GMT as it was reaching maximum intensity (fig. 2a). Photographs obtained near 2200 GMT, May 7 and 2100 GMT, May 8 show the cloud distribution in and near the vortex as the storm center weakened (figs. 3a, 4a). Satellite subpoints and principal points in the area viewed in these pictures are shown in figure 1, maps d, f and g, respectively.

Perhaps the most striking feature of the photographs is the degree of organization manifested by the spiral bands of clouds. These bands, which converge toward the "cloud crest" at A, give the viewer an immediate impression of a cyclonic circulation. Comparing figures 2a and 4a, it is apparent that in that length of time the number of bands associated with the storm decreased and the "crest" at A became more broken—a likely sequence of events considering the synoptic history of the vortex (fig. 1). However, it is interesting to note that even as the Low filled, the general pattern, or "cyclone print" [6], of the storm persisted throughout the period of decay. The persistence of the pattern between figures 3a and 4a, a time span of 23 hours, is quite remarkable.

The spiral bands associated with the vortex display a considerable dimensional variation—apparently unrelated to the vigor of the storm center. For example, the band DD′, figure 2a, measures about 600 n.mi. in length and varies in width from 15 to 30 n.mi. Close inspection of this band on the original positive transparency shows the main band to be composed of a number of smaller bands or streets. These component streets appear to vary in

605661—61——2

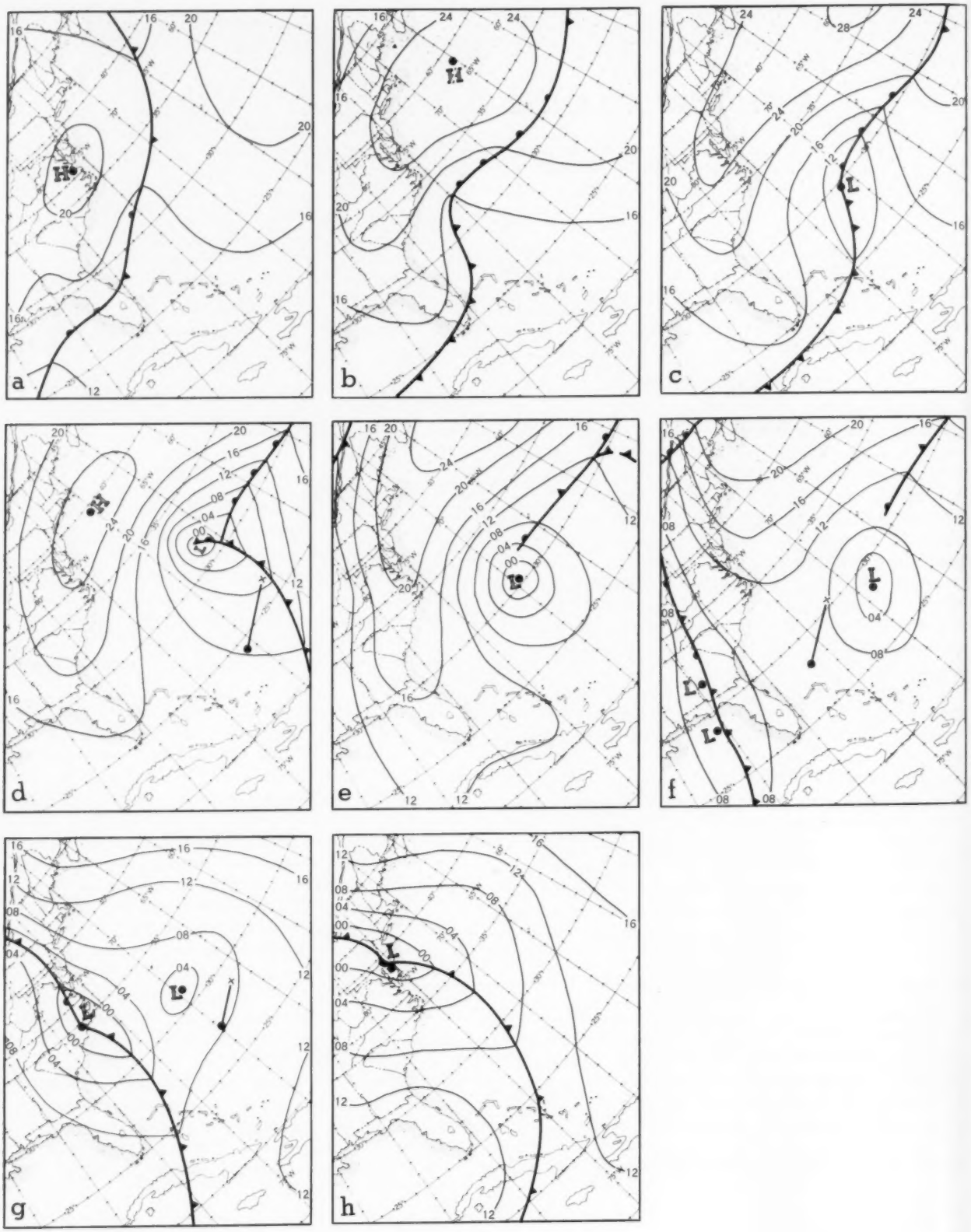
a
b
c
d
e
f
g
h

width from 3 to 10 n.mi.[1] The dimensional spectrum is displayed more graphically in figure 4a by comparison of bands II′ and JJ′. The latter is about 400 n.mi. long and varies from 15 to 60 n.mi. in width. The narrow band at II′, which measures about 2 n.mi. in width, appears to be continuous over a span of about 240 n.mi. It is conceivable that even narrower bands actually existed which are not visible in the photograph due to the limited resolving capability of the vidicon system [5].

In addition to the banded structure apparent in the pictures, another interesting feature is seen in figure 3a along FF′. Here the clouds are arrayed in the form of a chain with the cloud elements which form the links surrounding relatively cloud-free areas. Each link measures approximately 60 n.mi. in diameter with the inner, relatively cloud-free area measuring about 40 n.mi. Patterns similar to this "daisy chain" arrangement have been seen in photographs from the Atlas nose cone on August 11, 1959 [2], and in many pictures taken by TIROS [9]. The significance of this pattern is not immediately apparent though it may suggest the existence of a meso-scale convective regime.

The spiral banded structure of tropical storms has been well documented in the literature [4]. Pictures taken by TIROS I indicate that this banded organization may also be a common feature of the mature extratropical cyclone [7, 15, 6]. The organization apparent in the vigorous extratropical storm (fig. 2a) bears a striking resemblance to that of the typhoon seen near Australia on April 10 by TIROS I [13]. A mirror image of the typhoon is shown in figure 5 to facilitate comparison with the picture in figure 2a. (The mirror image reverses the clockwise sense of the Southern Hemisphere cyclonic circulation.) The relative positions and characteristics of the cloud images seen at A, C, and E as well as the spiral bands are features common to both storms.

SUBJECTIVE INTERPRETATION—CRITERIA AND COMPARISON WITH CONVENTIONAL DATA

Information derived directly from the pictures permits a reasonably accurate and detailed analysis of the organization and distribution of the clouds over most of the viewed area [5]. Information required to complete the description or nephanalysis of the picture—cloud form or type, probable thickness, and probable cloud top heights—must presently be subjectively inferred from the characteristics of the cloud images. Inferences drawn from synoptic models, and from relative brightness,[2] texture, size, shape, and edge characteristics of the cloud images presently form the somewhat tenuous basis for this subjective interpretation [1, 15].

Abbreviated station models showing total sky cover, cloud type, present and past weather, and sferics reports from data available for 0000 GMT on May 6, 8, and 9 are plotted on the appropriate view of the storm in figures 2b, 3b, and 4b for reference in the following interpretation of selected areas of the pictures.

The cloud mass at A in figure 2a, because of its lateral extent and amorphous character is interpreted to be an area of stratiform cloud. The brightness, relative to other cloud images in this picture, and the solid appearance of the area suggest that the clouds are dense, probably overcast and multilayered through the cirrus level. The extreme brightness of the image also suggests the possibility of imbedded convective cloud forms. In contrast, C in figure 2a is a relatively dull, featureless area which gives the impression of rather extensive, thin broken to overcast low stratiform cloud. In general, the spiral bands appear to be composed mainly of cumuliform cloud. This inference is drawn primarily from the small, relatively bright and sharply defined cloud masses within the bands (figs. 3a and 4a) and through reference to cyclone models. The band at JJ′ in figure 4a is reminiscent of the instability lines frequently observed in northwesterly flow to the rear of a cyclone center.

The small, bright, sharply defined cloud masses at E in figure 2a give the impression of strong cumulus activity. This impression is heightened by the thin veil-like cloud at E′ giving the appearance of cirrus spissatus being blown off tops of cumulonimbus.

The scarcity of surface observations from the area of the vortex (figs. 2b, 3b, 4b) prevents a more than superficial comparison of conventional observations and those made by the satellite. The subjective interpretations of cloud form based on criteria mentioned earlier can be neither completely supported nor rejected from the conventional data at hand. Data available in this case tend to show that the relatively brighter areas in the pictures contain clouds and weather generally associated with vertical development or deep cloud layers: (fig. 2a: moderate showers at A, showers and swelling cumulus at B′, showers at D, and towering cumulus below and to the left of E; figure 3a: towering cumulus near F′ and above and to the left of F, towering cumulus and showers at G, squalls at H, and cumulonimbus at H′; figure 4a:

[1] These details, available in the film transparency, may not reproduce clearly in the illustration. Much of the picture is in the local twilight zone resulting in low contrast within the area of the photograph. Local time within the pictured area varies from about 1700 hours on the left to about 1845 on the right where the horizon appears to "melt away" in darkness.

[2] Relative brightness alone admittedly can be misleading. Neiburger [11] has shown that relatively thin stratus can be highly reflective and Fritz [8] shows that the albedo for a given cloud type can vary over a significant range. On the other hand, preliminary results of investigations by Conover and by member of the Meteorological Satellite Laboratory show that deep cloud masses—large cumuli and cloud masses producing steady rain—frequently correspond to the brighter images in the photograph.

FIGURE 1.—Synoptic history of the west Atlantic vortex. NAWAC surface analyses for (a) 0000 GMT, May 3 1960; (b) 0000 GMT, May 4, 1960; (c) 0000 GMT, May 5, 1960; (d) 0000 GMT, May 6, 1960 with satellite subpoint (●) and picture principal point (+), for the picture in figure 2a; (e) 0000 GMT, May 7, 1960; (f) 0000 GMT, May 8, 1960 with satellite subpoint and picture principal point, for the picture in figure 3a; (g) 0000 GMT, May 9, 1960 with satellite subpoint and picture principal point, for the picture in figure 4a; and (h) 1200 GMT, May 9, 1960.

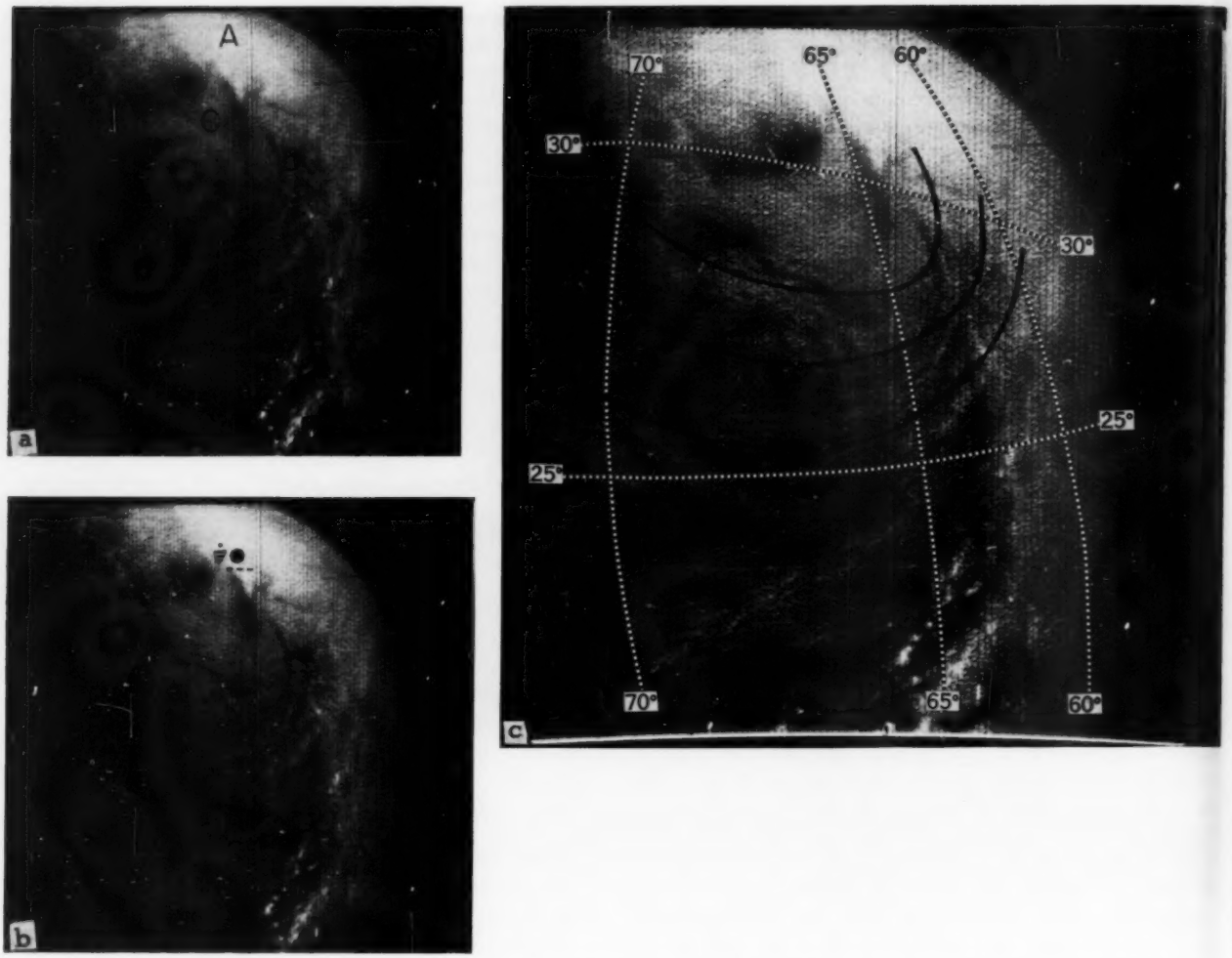

FIGURE 2.—(a) View of the vortex at 2200 GMT, May 5, 1960; (b) Same view with superimposed abbreviated station models from surface data for 0000 GMT, May 6, 1960; (c) Same view with latitude-longitude grid, and 1000–700-mb. mean flow superimposed.

altocumulus—altostratus at A and modreate to strong sferics returns at L). On the other hand, reports of fog, stratus, and stratocumulus—cloud forms and weather indicating little vertical thickness—appear to correspond to the relatively dark, amorphous cloud images in the photographs (fig. 2a: B,D′; fig. 3a: F). The report of clear skies at M in figure 4a corresponds to an area of the picture which is nearly black.[3]

4. RELATIONSHIP TO CONVENTIONAL ANALYSES

Kuettner [10] has shown that under certain conditions of stability and vertical wind distribution, cloud bands tend to parallel the direction of the flow in the convective layer. This relationship, if generally associated with cloud patterns identifiable from a satellite, would obviously enhance the meteorological value of the cloud pictures. For purposes of comparison, the mean flow between 1000 mb. and 700 mb., derived graphically from the surface and 700-mb. analyses prepared in NAWAC, is superimposed on the appropriate picture of the vortex in figures 2c, 3c, and 4c. In addition, latitude-longitude grids are superimposed to provide a familiar frame of reference [3]. Accepting the basic analyses as a good approximation of the flow pattern at the chosen levels—keeping in mind the inherent subjectivity—one finds a fair to good correlation between the orientation of the cloud bands to the south and west of the storm center and the mean contours delineating the flow to the rear of the cyclone within the 1000–700-mb. layer.

[3] Deep water normally appears black to the satellite unless specular reflection is present [8].

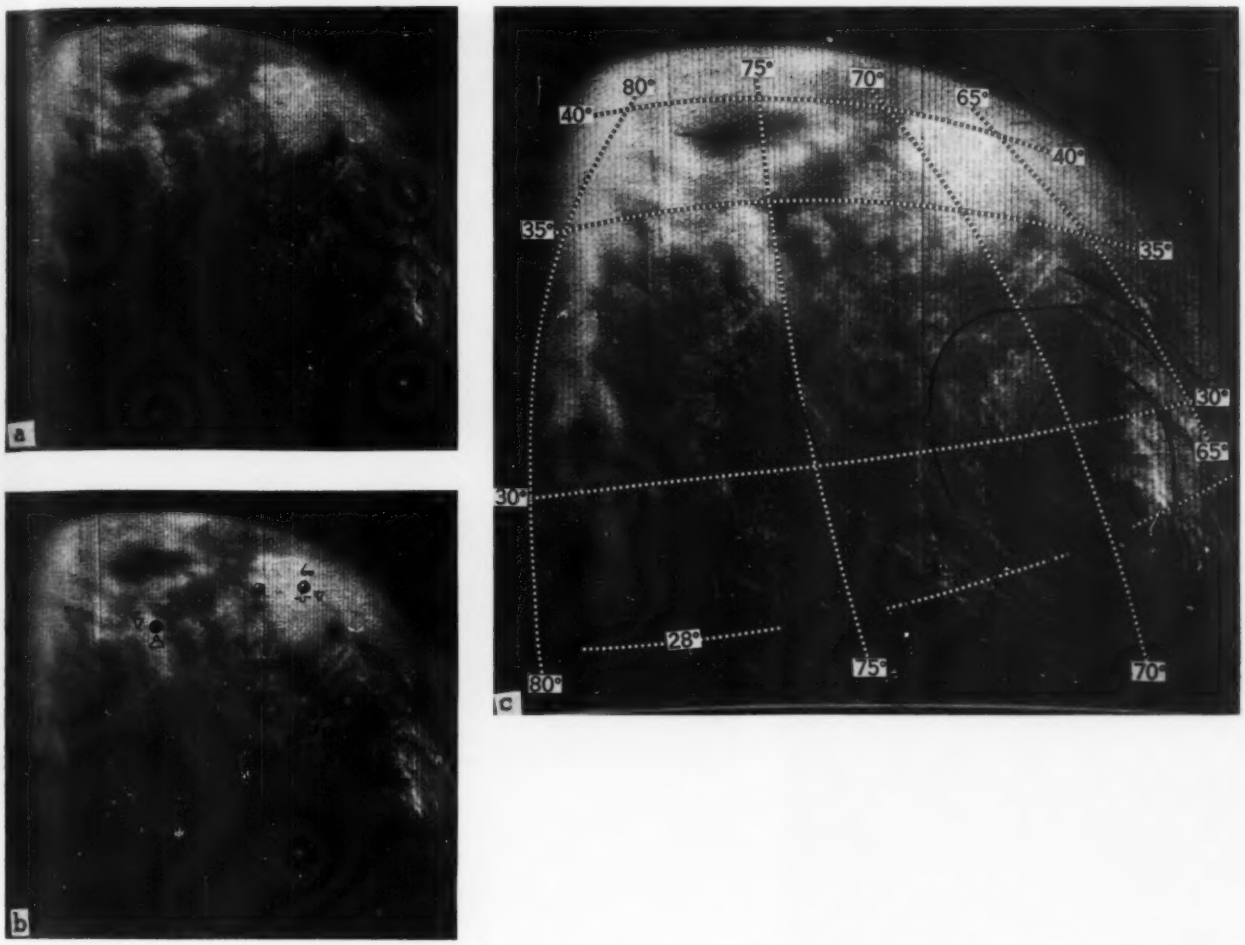

FIGURE 3.—(a) View of the vortex at 2200 GMT, May 7, 1960; (b) Same view with superimposed surface data for 0000 GMT, May 8, 1960; (c) Same view with latitude-longitude grid, and 1000–700-mb. mean flow superimposed.

5. OPERATIONAL UTILITY OF SATELLITE CLOUD PICTURES

The same lack of conventional weather data which frustrates a comprehensive study of this storm emphasizes the potential of a picture-taking satellite to provide useful observational data from areas where meteorological information in any form is either sparse or nonexistent.

The application of satellite cloud pictures to a routine analysis problem is demonstrated in figure 6. The shaded area in figure 6a reproduces an actual analysis of conventional cloud observations in terms of cloudiness significant for air operations in the middle troposphere. The majority of the data considered in this analysis are valid for 0000 GMT, May 9. The schematic nephanalysis from pictures over much of the same area taken approximately 3 hours earlier by TIROS I on pass 543 (fig. 4 represents one picture from this pass) is superimposed on the conventional analysis in figure 6b [14]. The abbreviated station models in figure 6a represent the total conventional data coverage within the area of "No Significant Cloud." It is apparent that an analyst relying solely on these data could not accurately depict the existing cloud distribution observed by TIROS. Yet it is conceivable that the areas of cumuliform cloud and the southward extension of the middle cloud deck at N in figure 6b are significant to the air operations mentioned above.

This series of pictures also provides an opportunity to apply satellite cloud information to the evaluation of a frontal analysis based on a few conventional observations and, of necessity, to a large extent on continuity. The picture in figure 2a represents the cloud pattern over the

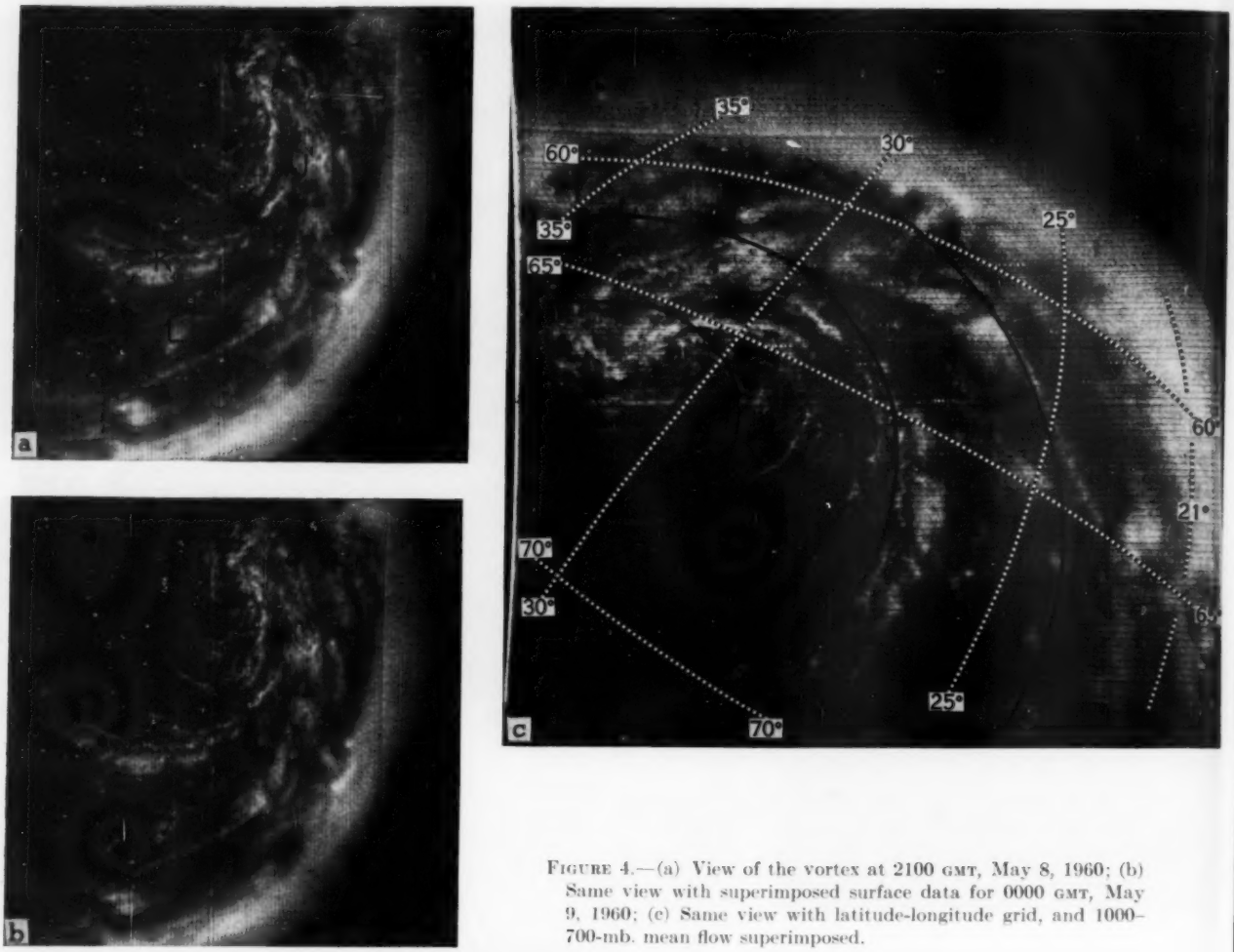

FIGURE 4.—(a) View of the vortex at 2100 GMT, May 8, 1960; (b) Same view with superimposed surface data for 0000 GMT, May 9, 1960; (c) Same view with latitude-longitude grid, and 1000–700-mb. mean flow superimposed.

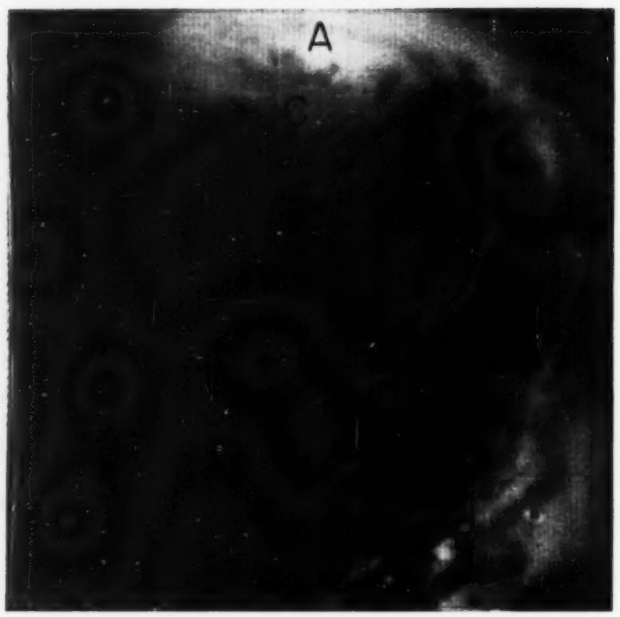

FIGURE 5.—Mirror image of the typhoon viewed by TIROS I near Australia on April 10, 1960 (for comparison of pattern with that of this vortex).

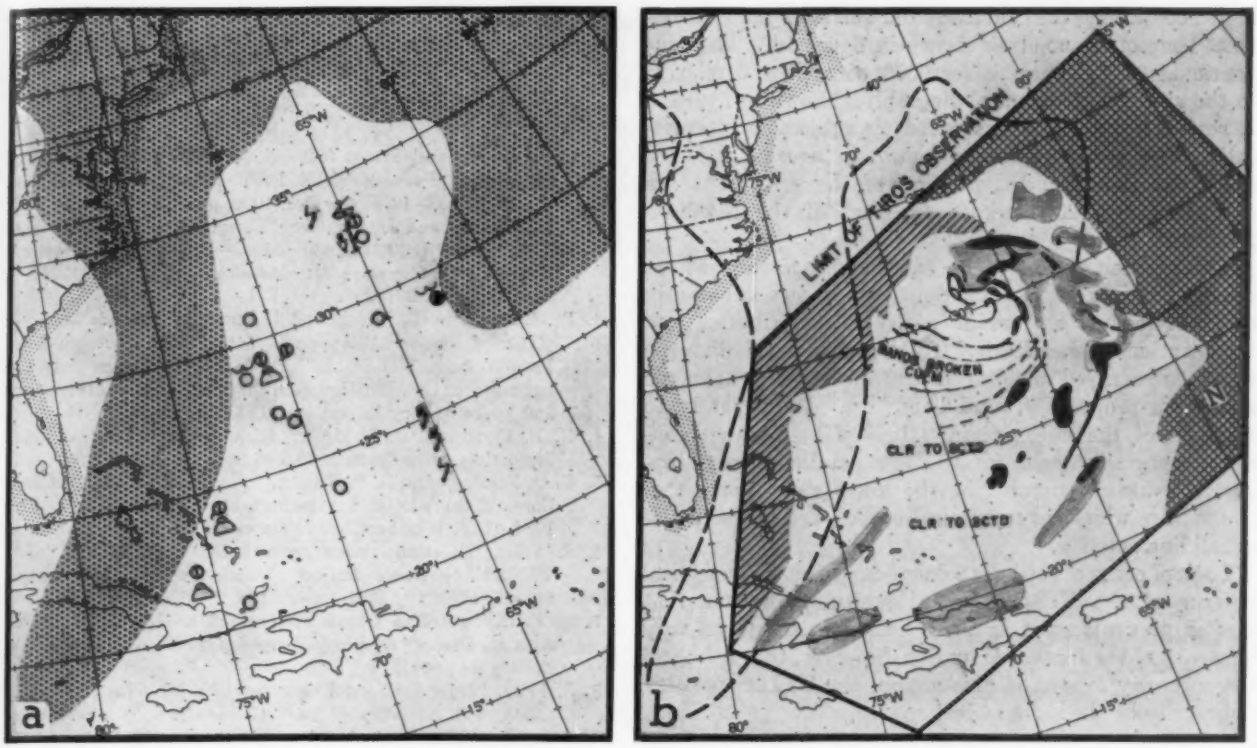

FIGURE 6.—(a) Nephanalysis of conventional cloud observations for 0000 GMT, May 9, 1960. Stippling shows broken to overcast cloud cover between 10,000 and 20,000 ft., no stippling indicates clear sky or scattered cloud between 10,000 and 20,000 ft. Abbreviated station models show conventional data available in the area of no significant cloud. (b) Nephanalysis made from TIROS I pictures for 2100 GMT, May 8, 1960. Dashed line shows extent of broken to overcast cloudiness on conventional nephanalysis of (a). Single-line hatching indicates broken to overcast clouds, type unknown; cross-hatching broken to overcast, probably mid-stratiform; solid shading indicates broken to scattered, probably large cumuliform; light shading broken to scattered, probably stratiform or small cumuliform.

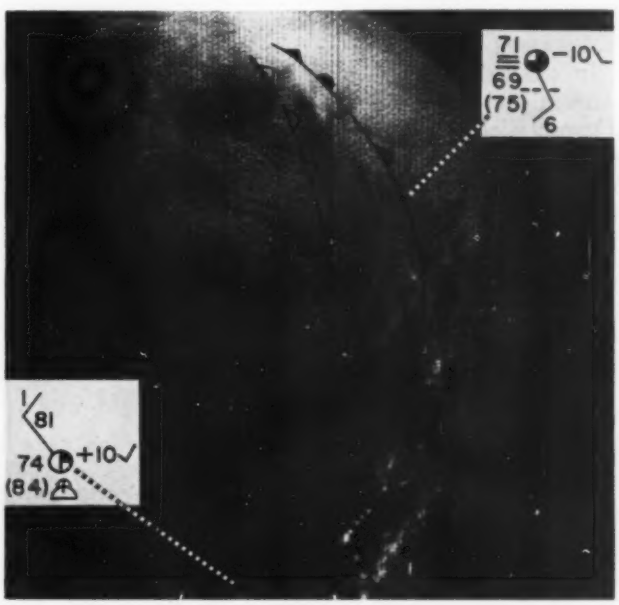

FIGURE 7.—View of the vortex at 2200 GMT, May 5 showing the NAWAC frontal position for 0000 GMT, May 6 (front with open symbols) with the two ship reports available to the analyst, and a proposed reanalysis of the front based on the conventional reports plus the picture data (front with solid symbols.)

region containing the cold front and vortex at the approximate time of the analysis shown in figure 1d. The conventional frontal analysis for 0000 GMT, May 6 relative to the appropriate cloud photograph is shown in figure 7. A revised frontal analysis based on subjective interpretation of the picture is also shown in figure 7. At its mid-point the amended position of the cold front lies approximately 120 n.mi. to the east of the NAWAC position.

The position suggested by the TIROS picture defines a boundary or zone of transition between two apparently different regimes as manifested by the distribution and organization of the clouds. To the west of this line the clouds are arrayed in spiral bands which tend to converge along the proposed frontal boundary. Immediately to the east of the line, generally broken to overcast conditions prevail except for the few parallel lines of apparently heavy cumulus in the lower right portion of the picture which, as mentioned earlier, are suggestive of squall line activity.

Lack of conventional data does not permit an analytical defense of the TIROS frontal position, and for that matter prevents even an analytical defense of the very existence of the front. Assuming, however, that a frontal discontinuity existed in this region, the TIROS position appears to be the more logical one.

6. SUMMARY

The TIROS pictures of the latter four days of this storm revealed a remarkable persistence in the organization of clouds associated with the vortex. The apparent decrease in numbers of spiral bands and the gradual breakup of the "crest" at A in figures 2, 3, 4 suggest that consecutive observations of the cloud patterns associated with a particular system at regular intervals may provide information regarding day-to-day changes of intensity and stage of development.

In discussing the relationship of the images to the conventional cloud observations, the subjectivity of the interpretation and the limitations thus imposed on practical applications are recognized. In spite of this subjectivity, which is also inherent to some degree in conventional weather observations, this study suggests that TIROS observations provide a basis for logical meteorological analysis in areas where conventional data are sparse or nonexistent.

REFERENCES

1. C. L. Bristor and M. A. Ruzecki, "TIROS I Photographs of the Midwest Storm of April 1, 1960", *Monthly Weather Review*, vol. 88, Nos. 9–12, Sept.–Dec. 1960, pp. 315–326.
2. J. H. Conover and J. C. Sadler, "Cloud Patterns as Seen from Altitudes of 250 to 850 Miles—Preliminary Results," *Bulletin of the American Meteorological Society*, vol. 41, No. 6, June 1960, pp. 291–297.
3. R. C. Doolittle, L. Miller, and I. Ruff, "Geographic Location of Cloud Features," Appendix 1 of "Some Meteorological Results from TIROS I," Staff, Meteorological Satellite Laboratory, U.S. Weather Bureau, in a National Aeronautics and Space Agency Report on TIROS I (in press).
4. G. E. Dunn and B. I. Miller, *Atlantic Hurricanes*, Louisiana State University Press, 1960, 326 pp. (pp. 152–173).
5. C. O. Erickson and L. F. Hubert, "The Identification of Cloud Forms from TIROS I Pictures" MSL Report No. 7, June 1961, (U.S. Weather Bureau manuscript).
6. S. Fritz, " 'Cyclone-Prints' from Satellite (TIROS I)," *INTERAVIA—World Review of Aviation and Astronautics*, vol. 15, 1960, pp. 1384–1385.
7. S. Fritz, "Satellite Cloud Pictures of a Cyclone Over the Atlantic Ocean," *Quarterly Journal of the Royal Meteorological Society* (in press).
8. S. Fritz, "Solar Radiant Energy and its Modification by the Earth and its Atmosphere," *Compendium of Meteorology*, American Meteorological Society, Boston, 1951, pp. 13–33.
9. A. F. Kreuger and S. Fritz, "Cellular Cloud Patterns Revealed by TIROS I," *Tellus*, (in press).
10. J. Kuettner, "The Band Structure of the Atmosphere," *Tellus*, vol. 11, No. 3, Aug. 1959, pp. 267–294.
11. M. Neiburger, "Reflection, Absorption, and Transmission of Insolation by Stratus Clouds," *Journal of Meteorology*, vol. 6, No. 2, Apr. 1949, pp. 98–104.
12. V. Oliver, "A Comparison of a Satellite Nephanalysis with a Conventional Weather Analysis for a Family of Pacific Frontal Storms," "Some Meteorological Results from TIROS I," Staff, Meteorological Satellite Laboratory, U.S. Weather Bureau, in a National Aeronautics and Space Agency Report on TIROS I (in press).
13. "TIROS I Completes Its Mission: TIROS II Readied," *Weatherwise*, vol. 13, No. 4, Aug. 1960, pp. 158–161.
14. W. K. Widger, Jr., "Examples of Project TIROS Data and Their Practical Use," *GRD Research Notes*, No. 38, July 1960.
15. J. S. Winston, "Satellite Pictures of a Cut-Off Cyclone over the Eastern Pacific," *Monthly Weather Review*, vol. 88, Nos. 9–12, Sept.–Dec. 1960, pp. 295–314.

BEHAVIOR OF THE PRINCIPAL HARMONICS OF SELECTED 5-DAY MEAN 500-MB. CHARTS

ROBERT L. HANEY

Extended Forecast Branch, U.S. Weather Bureau, Washington, D.C.

[Manuscript received April 13, 1961; revised June 22, 1961]

ABSTRACT

The coefficients A_n and B_n, and the percentage of the total height variance accounted for by each harmonic were computed for the first three longitudinal harmonics of 5-day mean 500-mb. height-contour charts at each 10° of latitude from 20° N. to 80° N. from December 1, 1959, to May 31, 1960. The phase angles and amplitudes of the first three harmonics were computed at 30° N., 50° N., and 70° N. and plotted as a function of time. Retrogression of the waves was found at high and low latitudes, while relatively stationary conditions prevailed at middle latitudes. The correlation coefficient between the contribution of the sum of the first three harmonics and the entire wave train was found to be almost +0.9.

1. INTRODUCTION

This is a report of a study of the behavior of the long waves of the atmosphere at the 500-mb. level and is part of a larger project designed to predict their movement and intensity.

The first step in this project, and the one with which this paper is largely concerned, is simply the observation of the movements and intensities of the three longest waves, in order to become familiar with their individual characteristics and climatological variations. Comparisons may then be made between their actual movements and those predicted by present methods. A careful investigation in terms of synoptic events may reveal methods by which the present forecasting techniques can be improved.

In this part of the project the Extended Forecast Branch's harmonic analysis program for the IBM 704 computer was used to compute the phase angles and amplitudes of each harmonic on 5-day mean 500-mb. height-contour charts using height profiles along selected latitudes during the 6-month period, December 1, 1959, to May 31, 1960. By an automatic data-processing method, height values were interpolated from twice-daily charts and 5-day means obtained thrice weekly at every 10° of longitude around the globe in the Northern Hemisphere. It is estimated that the resulting 5-day mean heights should be accurate to the nearest 30 feet.

2. HARMONIC ANALYSIS PROCEDURE

A good discussion of harmonic analysis may be found in Panofsky and Brier [1]. Some aspects of this technique will be repeated here in order to make clear what was done.

A finite sum of sine and cosine terms is found which together add up to the height variations at 36 grid points along a given latitude circle. The first harmonic (wave 1) has a wavelength of 360° longitude or the entire distance around the earth. This is called the "fundamental wavelength." The second harmonic (wave 2) has a wavelength equal to one-half the fundamental wavelength, or 180° longitude. The third harmonic has a wavelength equal to one-third the fundamental wavelength, or 120°, and so forth. The phase angle and amplitude of each harmonic were computed for every 10° of latitude from 20° N. to 80° N.

If N is the number of height values around a given latitude circle (36 in this case), there can be only $(N/2)-1$ sine harmonics and $N/2$ cosine harmonics. The sum of the entire series is given by

$$z=\bar{z}+\sum_{n=1}^{n=(N/2)-1}[A_n \sin n\lambda]+\sum_{n=1}^{n=N/2}[B_n \cos n\lambda] \qquad (1)$$

where z is the height value at any longitude (λ); $\bar{z}$ is the zonal average height; n is the wave number; and A_n and B_n are amplitude factors. This equation states that a local height value z is equal to the mean zonal height plus the sum of all harmonics.

For each given 500-mb. 5-day mean chart the coefficients A_n and B_n were obtained for each wave number n, until their sum explained 99 percent of the total height-variance (not necessarily from $n=1$ to $n=N/2$). This was done for each 10° of latitude from 20° N. to 80° N.

Once the coefficients A_n and B_n have been found for wave number n, its amplitude (C_n) is given by

$$C_n=\sqrt{A_n^2+B_n^2} \qquad (2)$$

and its phase angle by

$$\lambda_n=\frac{1}{n}\arctan(A_n/B_n) \qquad (3)$$

605661—61——3

The phase angle is measured in degrees longitude west of Greenwich and indicates the first position at which the wave-number n is at a maximum deviation; i.e., it marks the first ridge position. Since arctan (A_n/B_n) has two values between 0° and 360°, the correct choice of angle must be decided from the additional expression:

$$\lambda_n = \frac{1}{n} \arcsin (A_n/C_n) \qquad (4)$$

It is important to know what percent of the total variance explained by *all* the waves is explained by each *individual* wave. Since the harmonics are all uncorrelated, no two harmonics can explain the same part of the variance of the sample. Therefore, the variances explained by the different harmonics can be added. For example, if wave 1 accounts for 40 percent and wave 2 for 20 percent, then waves 1 and 2 combined account for 60 percent of the total variance. The equation for the variance of a single harmonic n is $C_n^2/2$, except for the last harmonic in the series for which it is C_n^2. If S_z^2 is the variance of the entire sample, then the percentage of the total variance which is explained by wave n is $C_n^2/2S_z^2$ when $n<N/2$.

3. CHARACTERISTICS OF THE VARIOUS WAVES

In the following discussion, an attempt will be made to describe the characteristics of the long waves as found on 5-day mean 500-mb. maps using the three previously discussed parameters, i.e., the position and amplitude of the wave, and the percent of the total height variance explained by each wave. Graphs showing the first two of these features plotted as a function of time for waves 1, 2, and 3 at latitudes 70° N., 50° N., and 30° N. are shown in figures 1 through 9.

Before discussing each of these graphs, a few general remarks should be made. Continuity in time for the phase angle of each harmonic is established from thrice-weekly charts separated by intervals of two or three days. This presents no special problem when, during this time interval, the longitudinal displacement of the wave is small. However, occasionally the phase angle appears to "jump" over a large longitudinal range, as illustrated in figure 1 in December when the first harmonic moved 180° of longitude in 2 days (pentad 11 to pentad 12). In such cases it cannot be definitely established whether the phase angle moved westward or eastward. Only 5-day mean charts constructed at shorter time intervals could resolve this difficulty. In fact, it is not even certain that continuity can be established at all in these cases, for the jumps frequently occur when the amplitude is quite small, often (as in the case mentioned above) approaching the limiting accuracy of 30 feet. It is possible in these cases that the original wave component completely died out and a new one subsequently formed in a different location. A few of the interesting examples

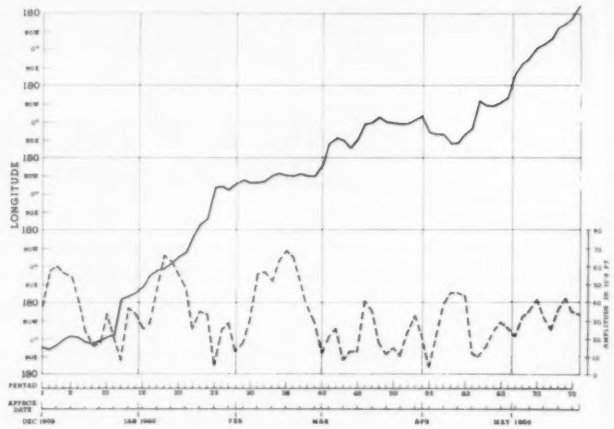

FIGURE 1.—Phase angle and amplitude of wave-number 1 at 70° N. as a function of time. Time scale (abscissa) is in consecutively numbered "pentads" rather than days. A pentad number is assigned in sequence to each 5-day mean 500-mb. chart used in computing the amplitude and phase angles. The time interval between consecutive midtimes of the overlapping 5-day means is either 2 or 3 days. Solid curve: phase angle in degrees longitude (scale at left). Dashed curve: amplitude in 10's of feet (scale at right).

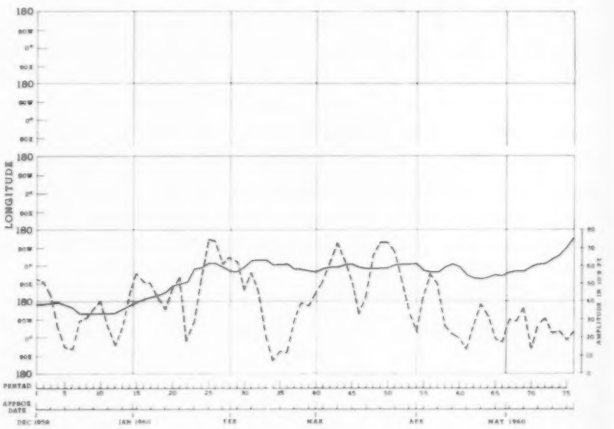

FIGURE 2.—Same as figure 1, except wave 2 at 70° N.

of such jumps will be included in the discussion of the individual graphs.

Figure 1 shows the phase angle and amplitude of wave 1 at 70° N. plotted as a function of time. This fundamental harmonic moved generally westward around the North Pole during the 6-month period beginning December 1, 1959 and ending May 30, 1960. During this period wave 1 made five complete revolutions around the Pole, averaging one every 5 weeks. One revolution in January, however, took only 3 weeks, and another in the spring, 8 weeks. Twice wave 1 remained stationary for at least 2 weeks, and on two occasions it progressed eastward for at least 1 week. In most cases the periods

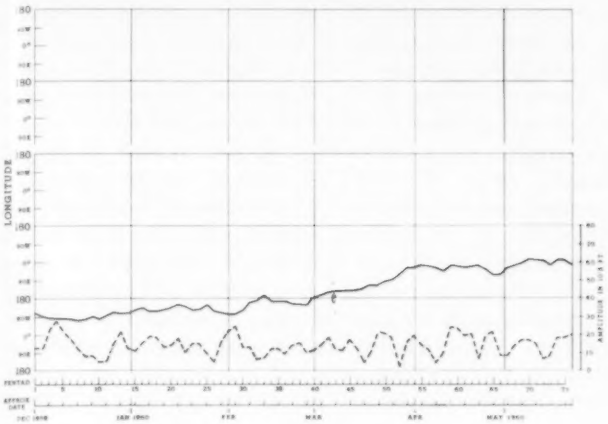

FIGURE 3.—Same as figure 1, except wave 3 at 70° N.

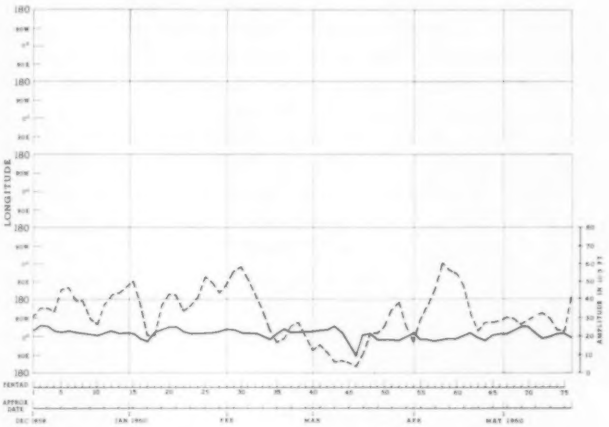

FIGURE 4.—Same as figure 1, except wave 1 at 50° N.

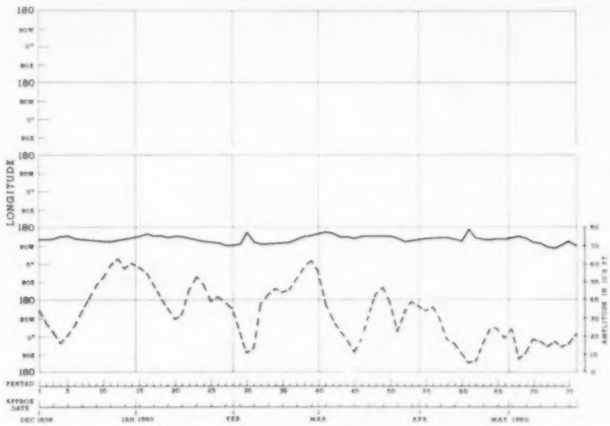

FIGURE 5.—Same as figure 1, except wave 2 at 50° N.

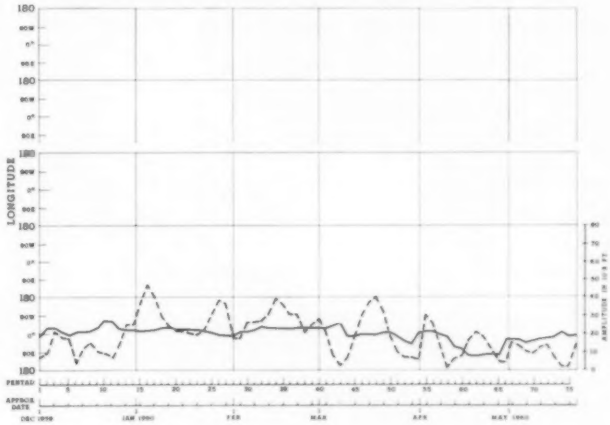

FIGURE 6.—Same as figure 1, except wave 3 at 50° N.

of rapid movement were associated with relatively low amplitudes, and slow movements were associated with relatively large amplitudes. In general, the amplitude was larger during the three winter months than during the three spring months. During the 6-month period, wave 1 at 70° N. explained, on the average, 39 percent of the total variance.

The steady westward movement which characterized wave 1 was clearly lacking in wave 2 at 70° N. (fig. 2). Two periods of slow steady retrogression (90° longitude per month) were observed—one during the first 3 weeks of January and the other from the end of April through the first 3 weeks of May. For 9 weeks beginning on January 21, wave 2 could be found within 15° east or west of Greenwich, and during the entire 6-month period it made only one revolution around the Pole. As with wave 1, the slower the movement, the larger the amplitude. During the few cases of progression the amplitude seemed to reach a minimum. At 70° N., wave 2 explained, on the average, 46 percent of the total variance, and waves 1 and 2 combined accounted for 85 percent of the total variance.

Wave 3 at 70° N. (fig. 3) showed less movement than either wave 1 or wave 2. During December and January it was relatively stationary near 90° or 100° W. During February and especially March, it retrogressed to 20° E. where it remained practically motionless for the next 2 months. During the three spring months, the amplitude curve tended to reach a small maximum every 9 to 14 days. On the average, wave 3 accounted for 10 percent of the total variance at 70° N. latitude. When combined, waves 1, 2, and 3 accounted for 95 percent of the total variance at 70° N. We should not expect this dominance of the lower wave numbers to persist as we move southward, because the distance around the globe increases at lower latitudes.

The persistent and rapid retrogression of the large-scale wave components at high latitudes during May has been

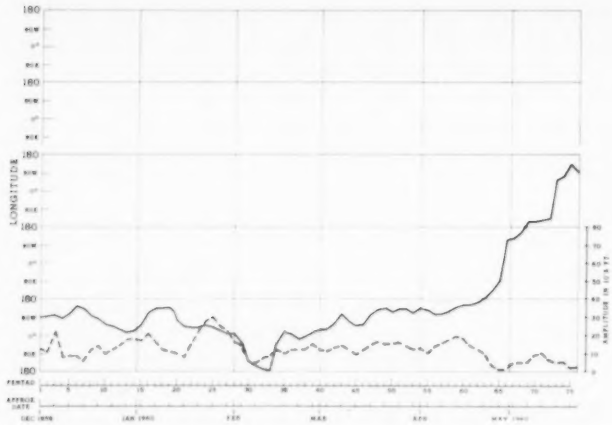

FIGURE 7.—Same as figure 1, except wave 1 at 30° N.

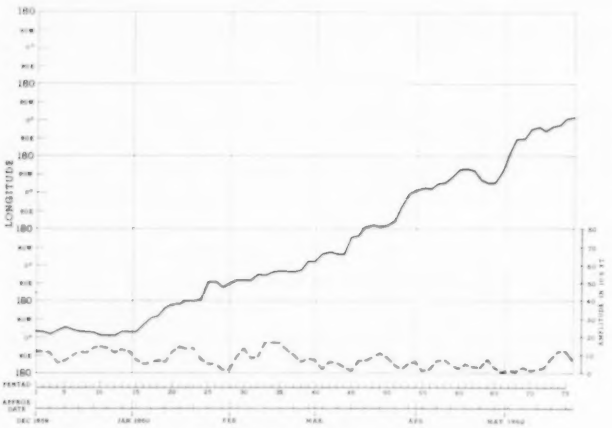

FIGURE 8.—Same as figure 1, except wave 2 at 30° N.

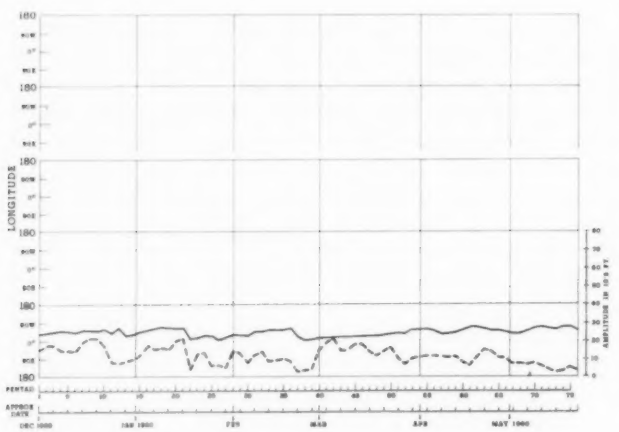

FIGURE 9.—Same as figure 1, except wave 3 at 30° N.

discussed by Andrews [2]. Evidently a period of equally pronounced retrogression of these wave components was present in January, as shown by figures 1 and 2.

Farther south at 50° N. there were no periods of persistent retrogression in any of the waves, and on the whole, the amplitudes, whether high or low, tended to persist longer. At 50° N. wave 1 (fig. 4) held a rather stationary position, passing back and forth across 0° Greenwich 17 times during the 6-month period, and only once did it move more than 20° east or west of it. On March 8, wave 1 started moving eastward and on the 5-day mean map near mid-month it had reached its most easterly position 100° E. More detailed studies may show a correlation between this marked eastward motion and the severe snow storms that lashed the east coast of the United States during the same period. Wave 1 at 50° N. accounted for, on the average, 33 percent of the total variance.

Compared to wave 1 at the same latitude, wave 2 (fig. 5) showed longer periods of slow persistent movement of the order of 25° longitude per month. This persistent movement generally lasted 3 to 4 weeks after which time the wave would reverse its direction for another 3 or 4 weeks. Twice during the period wave 2 seemed to jump rapidly westward, once in early February and again in mid-April. However, in both cases it returned just as quickly to near its original position. These two apparent "jumps" occurred at a time when the wave's amplitude had reached its two lowest values, and it is questionable whether or not they can be regarded as real. On the average, wave 2 accounted for 29 percent of the total variance at that latitude.

Wave 3 (fig. 6) showed more irregularities and rapid movements than either wave 1 or 2 at 50° N., although it was generally confined between 45° W. and 100° E. During the winter months (December, January, and February) it remained almost stationary near 10° W. From early March through the end of the period it was characterized by irregular eastward and westward movements, progressing as far east as 100° E. during April. Consistent with the other waves, little or no movement took place during the periods of relatively high amplitude, and the most rapid movements were associated with low amplitude. At 50° N., wave 3 accounted for, on the average, 12 percent of the total variance, and waves 1, 2, and 3 together accounted for 74 percent.

At 30° N., wave 1 (fig. 7) was characterized by alternating periods of slow and rapid movements. During the first 2½ months, wave 1 moved generally eastward from 90° W. to near 180°. During the 2 months that followed, wave 1 moved slowly westward back to near 100° W., after which the amplitude was so low that the wave's apparent movement no longer retained continuity or meaning. During this last month it accounted for only 11 percent of the total variance, whereas during the entire 6-month period wave 1, on the average, accounted for 24 percent of the total variance at 30° N.

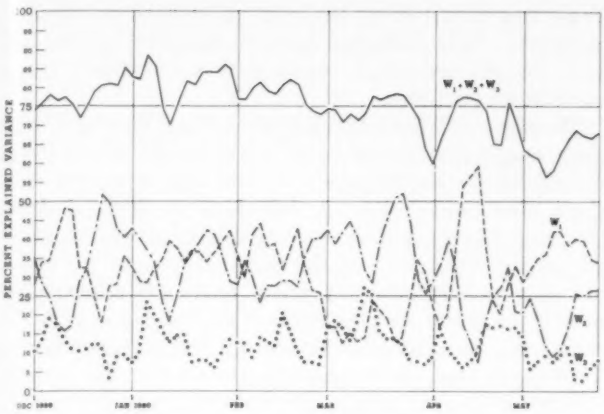

FIGURE 10.—Percentage of the total variance (ordinate) explained by wave 1 (dashed line), wave 2 (dash-dotted line), wave 3 (dotted line), and waves 1, 2, and 3 combined (solid line) at all seven latitudes (20° N., 30° N., . . . , 80° N.) as a function of time.

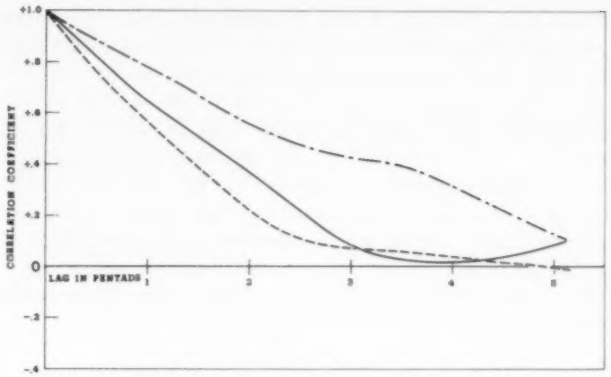

FIGURE 11.—Autocorrelation coefficient (ordinate) between phase angles of waves 1, 2, and 3 at 30° N., at time lags from 0 to 5 pentad numbers. A pentad number is assigned in sequence to each 5-day mean 500-mb. chart; the time interval between the midtimes of consecutive overlapping pentads is equal to 2 or 3 days. Solid line, wave 1; dashed line, wave 2; dash-dot line, wave 3.

The outstanding feature of wave 2 at 30° N. (fig. 8) was its continued westward movement around the globe. During the 6-month period, wave 2 completely circled the earth three times despite the fact that during the first month (December) it remained nearly stationary. Only twice did it move eastward for longer than a week. Since for the same angular velocity, the linear velocity at 30° N. is two and one-half times as great as it is at 70° N., wave 2 at 30° N. moved at about one and one-half times the speed of wave 1 at 70° N. On the average, wave 2 accounted for 11 percent of the total variance at 30° N.

Wave 3 (fig. 9) at 30° N. showed none of the irregularities of wave 1 nor the continued revolution around the earth which characterized wave 2. During the 6-month period it seemed to follow a pattern of very slow retrogression (35° longitude per month) followed by a rapid eastward motion (30° longitude per week) after which this apparent cycle was repeated again. During the entire period, wave 3 was located between 0° Greenwich and 80° W., and on the average it accounted for 22 percent of the variance. Waves 1, 2, and 3 together accounted for 57 percent of the total variance at 30° N.

Figure 10 shows the percentage of the total variance which was explained by wave 1 (dashed line); wave 2 (dash-dotted); wave 3 (dotted line); and waves 1, 2, and 3 combined (solid line) at all seven latitudes (20° N., 30° N., . . . , 80° N.) as a function of time. One can easily tell by looking at the solid curve that the three waves together accounted for a greater percentage of the total variance during the first three months than during the last three. Specifically, they accounted for 79.4 percent during the three winter months, and, on the average, only 70.2 percent during the three spring months.

It should also be mentioned that during periods of low

605661—61——4

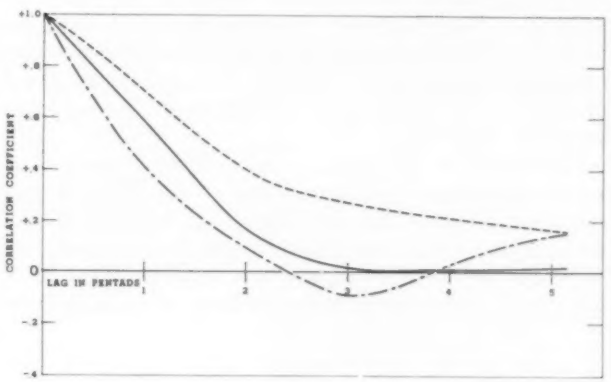

FIGURE 12.—Same as figure 11, except at 50° N.

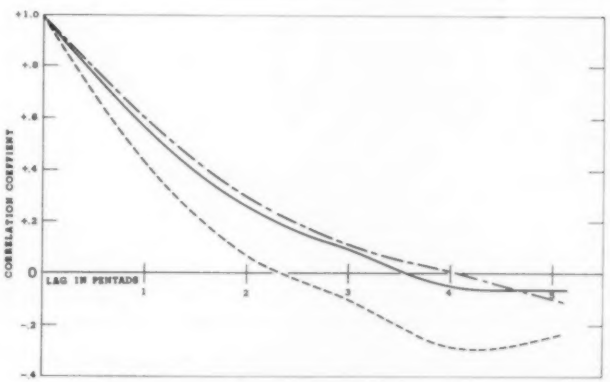

FIGURE 13.—Same as figure 11, except at 70° N.

zonal index, waves 1, 2, and 3 explained a relatively small percent of the total variance (end of March and first part of May) and during periods of high zonal index they explained a large percent of the total variance (mid-April).

Autocorrelations were computed for the phase angles of waves 1, 2, and 3 at 30° N., 50° N., and 70° N., and the correlograms are shown in figures 11, 12, and 13. It was hoped that a power spectrum analysis could be carried out on those waves which showed some possibility of periodicity (i.e., those whose correlograms do not fall away exponentially). However, time restrictions made this impossible.

4. CONCLUSIONS AND SUGGESTIONS FOR FUTURE STUDY

Eliasen's [3] study, using daily maps over a shorter time period, showed the semipermanence of the longest waves ($n=1$, 2, 3, and 4) at 50° N. An inspection of figures 1–9 reveals this semipermanence at mid-latitudes (50° N.) and also shows a tendency for retrogression of these long waves at high (70° N.) and low (30° N.) latitudes. The stationary character at middle latitudes may be, as Eliasen maintains, a consequence of the large mountain ranges, or it may be that baroclinic action counteracts the retrogression tendencies of the long waves at middle latitudes.

Inspection of the graphs reveals that there is little similarity between the movement of the different long waves at the same latitude. Eliasen [3], however, showed that during two fall months, there was great similarity between the motion of two short waves ($n=6$ and 7) at 50° N. The graphs also show that there is little correspondence of phase and amplitude of the long waves between adjacent latitudes. This indicates frequent sheering of full-latitude troughs and ridges rather than a concurrent movement at all latitudes.

The movements of the waves and the fluctuations of their amplitudes would be of greater significance if the corresponding climatological values were removed from these two parameters. A laborious method of doing this would be to perform an harmonic analysis on about 10 years of data and find the mean position of the waves for each particular 5-day mean chart. Similar results may be obtained by performing an harmonic analysis on the normal monthly and mid-monthly maps, interpolating for values near the beginning and end of the month. Finally, a power analysis of the correlograms after more lags have been computed might reveal further statistical characteristics of the movements of these long waves.

ACKNOWLEDGMENTS

I would like to thank all the members of the Extended Forecast Branch for the use of computational facilities time and for their gracious cooperation; and particularly Billy M. Lewis for his advice and guidance throughout the project.

REFERENCES

1. H. A. Panofsky and G. W. Brier, *Some Applications of Statistics to Meteorology*, The Pennsylvania State University, University Park, Pa., 1958, (pp. 128–134, 138–144).
2. J. F. Andrews, "The Weather and Circulation of May 1960—Including a Discussion of the Unusual Retrogression of 5-Day Polar Vortices," *Monthly Weather Review*, vol. 88, No. 5 May 1960, pp. 193–202.
3. E. Eliasen, "A Study of the Long Atmospheric Waves on the Basis of Zonal Harmonic Analysis," *Tellus*, vol. 10, No. 2., May 1958, pp. 206–215.

RELATIVE CATCHES OF SNOW IN SHIELDED AND UNSHIELDED GAGES AT DIFFERENT WIND SPEEDS

LEONARD L. WEISS

Hydrologic Services Division, U.S. Weather Bureau, Washington, D.C.

[Manuscript received June 15, 1961]

ABSTRACT

Some results are presented of a comparison of the observations of precipitation catch in pairs of standard 8-inch gages, one equipped with an Alter-type windshield and the other unshielded. The ratios of the catches of snow vary with the average daily wind speed. A generalized wind speed-catch ratio relationship based on previously reported observations is included.

1. INTRODUCTION

The precipitation gage catch is one of the primary items of observation in meteorology, hydrology, and climatology. How well the individual gage performs its task of measuring the amount of precipitation has been of concern since Heberden [2] found that similar gages close to each other but at different heights above the ground gave different catches.

Subsequent investigators have demonstrated that the gage performs its task less and less efficiently as the wind speed increases. In addition, at any given wind speed, the deficiency of catch increases greatly from the case of large raindrops to that of fine, dry snowflakes.

Many attempts have been made to devise protective shields which would eliminate the adverse effect of wind on the catch. None has been entirely successful. The two most practical and widely used are the rigid shield devised by Nipher [3] or a variant of it, and the flexible one devised by Alter [1] or a variant of it. The former is of trumpet-shape with flared end upward and at the level of the gage orifice. The latter is of similar shape but consists of loosely hung, movable metal strips. The Alter, or flexible type, is superior to the rigid type and has come into general use in the United States. The results of previously reported investigations of influence of wind speed on gage catch were summarized and an extensive bibliography was given by Weiss and Wilson [5].

Of those previously reported investigations, only two, Long [4] and Alter [1], compared directly the catch of an unshielded gage with that of a gage with flexible shield. In each of these cases the wind observations were not at the gage orifice. In the latter case they were seven miles away.

The aim of this report is to present the results of a comparison of the observations of catch of snow in four pairs of gages, one of each pair equipped with a flexible shield. The ratios of the catches of each pair are found to vary with the average wind speed. The anemometers were placed nearby and at the orifice level of the gages. The results are found to be in accord with general relationships based on the work of previous investigators.

FIGURE 1.—Location of precipitation stations.

2. DATA USED

The data were obtained from the RH-4 Northeastern Lake Michigan precipitation project, a joint project of the Corps of Engineers, U.S. Lake Survey, and the U.S. Weather Bureau. The four Michigan stations used in this comparison are: Elberta, Mackinaw City, Manistique Water Works, and St. James, Beaver Island. Totalizing anemometers were installed in January 1956. The exposures were open with woods no closer than 100 feet in any case. Beaver Island is in the northern part of Lake Michigan, and the other three stations are on the shore of the northeastern end of the lake. All four are within a radius of 60 miles. The station locations are shown on the map of figure 1. The climatological record indicates that in this region the normal daily maximum temperature drops to freezing (32° F.) near the first of December and remains below until near mid-March. The normal daily average temperature drops to freezing by mid-November and remains below to about the first of April.

The data consist of daily observations at each station of maximum and minimum temperature, daily precipitation catch in the standard 8-inch gage, daily precipitation catch in an additional standard 8-inch gage equipped with an Alter-type flexible shield, and the daily wind movement in miles indicated by a totalizing anemometer. The anemometer was mounted near the gages with the bottom of the cups level with the gage orifice.

The data forms were filled out once per day by the observers. Since the character of the precipitation was not recorded, it is not known whether the catch was of snow or rain or a mixture. It is known that the influence of wind speed on the catch is much greater for snow than for rain. Also that when the temperature is below freezing, the precipitation is almost certain to be snow. For those reasons, the criterion was used that the catch was assumed to be snow if it occurred on a day on which the maximum temperature was freezing (32° F.) or below.

The observer reported the totalizing anemometer reading at the regular observation time. The daily wind movement is found by subtracting the previous day's reading. This difference divided by 24 gives the average hourly wind speed in miles per hour. This method, of course, masks the peak values of wind speed and increases the scatter of the plotted points when catch ratio of unshielded to shielded gages is plotted versus the wind speed. For this study, data used were for the period from the time of installation of the anemometers in January 1956 through December 1958. Only those cases were used for which the catch of the unshielded gage was more than 0.01 inch. For Elberta, there were 73 cases; Mackinaw City 45; Manistique 50; and St. James, Beaver Island 37.

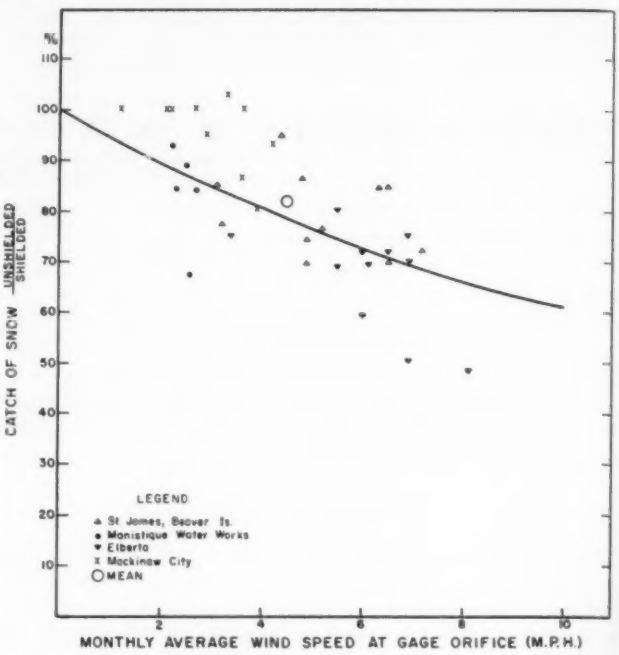

FIGURE 2.—Relation between monthly average wind speed (m.p.h.) at gage orifice and ratio of snow catch in unshielded to shielded precipitation gages. Data from February 1956 to December 1958, inclusive.

3. ANALYSIS OF THE DATA

Table 1 gives the ratio of the 5-year average catch of the unshielded gage to that of the shielded gage for the four stations mentioned above plus Charlevoix for the period 1954–1958. The latter station was not included in the rest of the analysis because of incomplete wind data.

The marked difference in the ratios for the part of the year when the temperatures are below freezing is an indication of the more deleterious influence of wind on the unshielded gage catch in case of snow. It is also a reflection of the improved catch of snow when the gage is equipped with the shield. The effect of the shield is less pronounced during that part of the year when the precipitation is usually rain.

For the four stations of this study, the ratios of the monthly total unshielded gage catch to that of the shielded gage for the months of December, January,

TABLE 1.—*Ratio (in percent) of unshielded to shielded gage precipitation catch. Data from five stations, 1954–1958.*

	Jan.	Feb.	Mar.	Apr.	May	June	July	Aug.	Sept.	Oct.	Nov.	Dec.
Unshielded / Shielded (average %)	82	83	84	99	99	99	99	99	99	99	96	84
				temperatures above freezing								

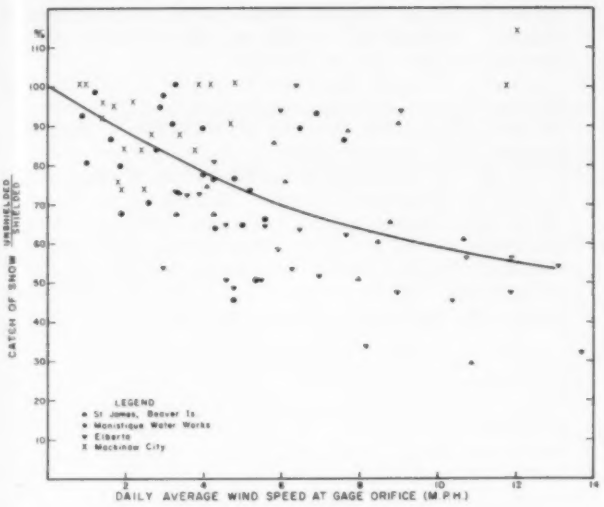

FIGURE 3.—Plot of daily ratio of unshielded to shielded gage catch of snow against daily average wind speed for cases when shielded gage catch ≥ 0.10 inch.

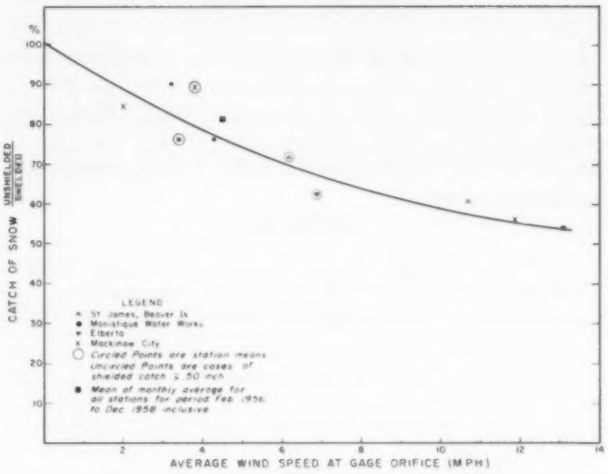
CATCH OF SNOW UNSHIELDED / SHIELDED
%
LEGEND
St James, Beaver Is.
Manistique Water Works
Elberta
Mackinaw City
Circled Points are station means
Unircled Points are cases of shielded catch ≥ 50 inch
Mean of monthly average for all stations for period Feb 1956 to Dec 1958 inclusive
AVERAGE WIND SPEED AT GAGE ORIFICE (M.P.H.)

FIGURE 4.—Plot of mean ratios (unshielded to shielded gage catch) against average wind speed.

February, and March when the precipitation could be considered to be mostly snow, were plotted versus the monthly average wind speeds. This wind speed was found by dividing the monthly anemometer totals of miles of wind by 24 hours times the number of days in the month. The data are plotted in figure 2. They suggest a decrease in the ratio with increasing wind speed for snow.

The plots of individual day ratios versus daily average wind speed for those cases where the daily maximum temperature did not exceed 32° F., and the unshielded gage catch was more than 0.01 inch show a large scatter which is probably partly due to the variability of the wind speed. This variability can be obscured in the daily average. In addition there is a large ratio variation when the catch is small. The scatter can be reduced somewhat and the trend made more apparent if only those cases are included where the unshielded gage catch is greater than 0.10 inch. These cases for all four stations are plotted in figure 3. Two of the points (for Mackinaw City) lie far from the general trend line. Both of these cases occurred during the first winter of record. When the shields were first installed they were placed with their tops several inches above the orifice of the gages. In September 1956, all the shields were lowered to set the tips of the blades one-half inch above the gage orifice.

To delineate the relationship further, mean values for the total period at each station and the individual cases where the daily shielded catch value was 0.50 inch or more are plotted in figure 4. A curve drawn to these points is considered to best express the inherent relationship between the catch ratio and wind speed.

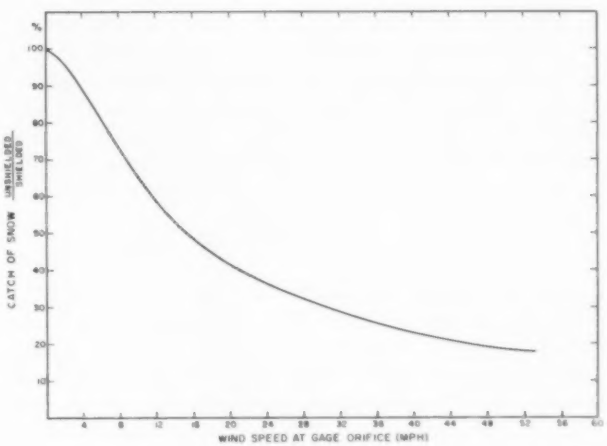

FIGURE 5.—Generalized relationship between the ratio of snow catch (unshielded to shielded gage) and wind speed at gage orifice, based on data of previous investigators.

4. COMPARISON WITH PRIOR WORK

A generalized relationship between the ratio of the unshielded to shielded gage catch of snow and the wind speed at the gage orifice is shown in figure 5. This curve is based on data given by the various investigators listed in the references of Weiss and Wilson [5].

The results of this investigation expressing the catch ratio—wind speed relation as determined from the Michigan station data, figure 4, show good agreement with the comparable portion of the general relationship curve of figure 5.

ACKNOWLEDGMENTS

I wish to thank R. F. Kresge, Eastern Area Hydrologic Engineer, for his cooperation in making available RH—4 project data, for helpful discussion, suggestions, and general encouragement during this study, and A. L. Shands, T. J. Nordenson, and J. L. H. Paulhus for reviewing the final draft.

REFERENCES

1. J. C. Alter, "Shielded Storage Precipitation Gages," *Monthly Weather Review*, vol. 65, No. 7, July 1937, pp. 262–265.
2. W. Heberden, "Of the Different Quantities of Rain, Which Appear to Fall at Different Heights, Over the Same Spot of Ground," *Philosophical Transactions*, Royal Society of London, vol. 59, Dec. 1769, pp. 359–362.
3. F. E. Nipher, "On the Determination of the True Rainfall in Elevated Gages," *Proceedings of the American Association for the Advancement of Science*, vol. 27, 1878, Salem, Mass., pp. 103–108.
4. T. L. Long, "A Comparison of Snowfall Catch in Shielded and Unshielded Precipitation Gages, "*Bulletin of the American Meteorological Society*, vol. 28, No. 3, Mar. 1947, pp. 151–153.
5. L. L. Weiss and W. T. Wilson, "Precipitation Gage Shields," *Extrait des Comptes Rendus et Rapports—Assemblée Général de Toronto 1957*, Tome I, International Union of Geodesy and Geophysics, Gentbrugge, 1958, pp. 462–484.

A COMPARISON OF METHODS FOR COMPUTING DAILY MEAN VALUES OF DRY BULB TEMPERATURE, DEW POINT, AND RELATIVE HUMIDITY

MILTON L. BLANC

Office of Climatology, U.S. Weather Bureau, Washington, D.C.

[Manuscript received May 3, 1961]

ABSTRACT

This study compares several methods of computing daily mean values of dry bulb temperature, dew point, and relative humidity. Data are daily observations at nine selected points in the contiguous United States for 5 years of record during the mid-season months of January, April, July, and October. Daily mean values of the three elements were computed from the four synoptic observations (sum÷4) and from the 24 hourly observations (sum÷24). Also, for dry bulb temperature and dew point, they were computed from the daily highest and lowest hourly value (sum÷2). With the mean of the 24 hourly values as the base, daily departures of the means computed by the other methods were determined. Averages and standard deviations of these daily departures were computed for each station-month for the 5-year period. These were mutually compared, with the conclusion that when the methods tested are applied to dew point and relative humidity, the departures from the 24-hour mean are generally no larger, and in many cases are smaller, than those obtained in computing daily mean dry bulb temperature by the same method.

1. INTRODUCTION

A new format for the Weather Bureau's *Local Climatological Data* (*Supplement*) was introduced with the issue dated January 1961. Table G of the new format lists daily values of 24-hour averages of several elements including dry bulb temperature, dew point temperature, and relative humidity. These values are computed by adding the 24 values entered at each record hourly observation and dividing the sum by 24. This source makes daily 24-hour means of these elements available from over 200 Weather Bureau stations in the United States. At most of the same stations, daily values of mean temperature obtained by the usual method of taking one-half the sum of the maximum and minimum are published in the corresponding *Local Climatological Data*.

Decision to publish these new data was, in part, in response to the growing interest in and demand for daily mean values of dew point and relative humidity. Much of this demand comes from agronomists and hydrologists who are interested in computing evaporation and evapotransipiration [1, 2, 3]. The published data will be useful but the number of stations and periods of record for which they are available are limited. For studies or investigations involving other stations or locations or periods of record it will be necessary to use daily mean values based on the mean of the maximum and minimum or the mean of the four "synoptic" observations. Van Bavel and Verlinden [2] use mean relative humidity from the four synoptic observations (one every six hours). Newman, Shaw, and Suomi [3] propose simple instrumentation to obtain daily maximum and minimum dew point temperatures at agrometeorological observing stations.

A great deal has been written about the relative merits of computing daily mean temperatures according to various formulas [4, 5, 6]. However, the question of computing daily mean values of dew point or relative humidity has not been similarly treated. The purpose of this present study is to compare several common methods of computing such daily means as they apply to dew point and relative humidity.

2. DATA USED

Nine stations in the contiguous United States were selected for this study. Data for the mid-month of each season (January, April, July, October) were processed for five years of record (1955–1959). The following computations were made for each day of the five years for each station month:

(1) Dry bulb temperature (° F.).
   a. daily mean of 24 hourly values (sum÷24).
   b. daily mean of 4 "synoptic" observations (sum÷4).
   c. daily mean of highest and lowest hourly values (sum÷2).
   d. daily difference between a and b and between a and c.

(2) Dew point temperature (° F.).
   a. daily mean of 24 hourly values (sum÷24).
   b. daily mean of 4 "synoptic" observations (sum÷4).
   c. daily mean of highest and lowest hourly values (sum÷2).
   d. daily difference between a and b and between a and c.

(3) Relative humidity (percent)
   a. daily mean of 24 hourly values (sum÷24).
   b. daily mean of 4 "synoptic" observations (sum÷4).
   c. daily difference between a and b.

The daily means were rounded to one decimal to determine the daily differences which were then rounded to whole numbers. These daily differences (1d, 2d, and 3c) for each month at each station for the five years were then accumulated in a frequency table. The class intervals were 1° F. for dry bulb and dew point temperatures and 1 percent for relative humidity. Percent frequencies were computed for each class. In all cases the daily mean of the 24 hourly values was taken as the "true" mean (Conrad and Pollak [4]) from which to determine the daily departures. In addition, for each station-month, the mean departure and the standard deviation of the daily departures were determined.

These results (mean departure and standard deviation) for each comparison for each station-month are summarized in tables 1 to 5. In addition, for three of the stations, the percent frequency distribution of daily departures from the "true" mean are presented in graphical form (figs. 1, 2, and 3). For this purpose, one west coast station (San Francisco), one continental station (Bismarck), and one east coast station (Washington) were selected. In these figures, the class interval (abscissa) for dry bulb temperature and dew point is 1° F. For relative humidity, the class interval is 3 percent (See Appendix).

It was also considered desirable to examine the shape of the diurnal curves of hourly values of these elements. Average hourly temperatures (dry bulb) for a number of stations are available in the "Climatological Record" books formerly kept on station. The average curves for these four months for the same three stations are given in figures 4, 5, and 6 with the highest and lowest values shown.

Average hourly values of dew point and relative humidity are not available from this source for these stations. However, the average curves for the month of January 1961 (the first month of publication of the new *Supplement*) are presented in figures 7, 8, 9. Here the curves for all three elements are presented on the same graph to facilitate comparison.

In addition to the average monthly curves, it was of interest to examine the daily march of these elements on individual days selected to represent some departure from the average. The standard deviations in tables 1 and 2 indicate a considerable variability in the daily departures at Bismarck in January, although the average departure is very small. The frequency of air mass changes at this continental location in winter is one of the principal reasons for this large variability. Therefore, four dates in January 1961 at Bismarck were selected as examples of the types of unusual daily curves which may occur. They are presented in figure 10.

3. DISCUSSION

As stated in the introduction, a principal purpose of this study was to examine and compare several methods of computing daily mean values of dew point and relative humidity. However, to give these comparisons a "common denominator" familiar to climatologists and others accustomed to handling temperature data, the results are presented against a background of similar computations and comparisons of daily mean dry bulb temperature. These latter have been frequently studied [4, 5, 6] and the limitations of the various methods of computation are fairly well known. Therefore it was felt that by using dry bulb, dew point, and relative humidity data from the same stations for the same months and periods of record, the usefulness of the study would be greatly increased.

TABLE 1.—*Dry bulb temperature: synoptic mean vs. 24-hr. mean. Average departure of mean of 4 synoptic observations from 24-hr. mean and standard deviation of daily departures. 5 years of record, °F.*

Station	January		April		July		October	
	Dep.	S.D.	Dep.	S.D.	Dep.	S.D.	Dep.	S.D.
Seattle	+0.1	0.4	+0.2	0.5	−0.1	0.6	+0.2	0.5
San Francisco	+0.5	0.6	+0.3	0.5	+0.3	0.4	+0.4	0.6
Salt Lake City	+0.3	1.1	+0.3	1.1	−0.3	1.0	+0.6	1.2
Bismarck	+0.1	1.4	0	1.1	−0.2	0.9	0	1.3
Fort Worth	0	1.1	−0.1	1.1	−0.1	0.7	−0.2	0.9
St. Louis	0	1.3	−0.2	1.1	−0.1	0.8	−0.3	1.0
Boston	0	0.7	−0.1	0.7	0	0.7	−0.2	0.6
Washington	−0.1	0.7	−0.2	0.8	0	0.5	−0.2	0.6
Miami	−0.4	0.7	−0.4	0.6	−0.2	0.7	−0.4	0.6

TABLE 2.—*Dry bulb temperature: mean of high/low vs. 24-hr. mean. Average departure of mean of highest and lowest hourly from 24-hr. mean and the standard deviation of daily departures. 5 years of record, °F.*

Station	January		April		July		October	
	Dep.	S.D.	Dep.	S.D.	Dep.	S.D.	Dep.	S.D.
Seattle	+0.1	0.8	+0.2	0.9	+0.4	1.1	+0.3	0.9
San Francisco	+1.0	1.0	+0.8	1.1	+1.7	1.0	+1.5	1.3
Salt Lake City	+0.5	1.4	0	1.3	−0.9	1.3	+0.6	1.3
Bismarck	+0.1	1.9	−0.1	1.3	−0.1	1.3	+0.9	1.6
Fort Worth	+0.4	1.6	+0.1	1.2	+0.2	1.0	+0.1	1.0
St. Louis	−0.1	1.3	+0.1	1.3	+0.2	1.0	+0.4	0.9
Boston	0	1.4	+0.6	1.2	+0.4	1.1	+0.1	1.1
Washington	+0.4	1.1	+0.2	1.2	+0.3	1.1	+0.4	0.9
Miami	+0.1	2.1	+0.1	0.8	+0.3	1.0	+0.4	0.8

DRY BULB TEMPERATURE

Tables 1 and 2 present the results of comparing daily mean temperatures computed from the four synoptic observations and from the daily highest and lowest hourly readings with the "true" 24-hour mean. The computations are based on five years of record for each station-month. The first column under each month lists the average daily departure from the "true" mean. The second column presents the standard deviation of the daily departures. When the average departures and standard deviations in table 1 are compared with those in table 2, a measure of the relative reliability of these two short-cut methods is disclosed. In table 1 there are only 2 cases in which the average departure (ignoring sign) equals or exceeds 0.5° F., while in table 2 there are 9 such cases. In table 1, only 10 out of 36 (26 percent) of the standard deviations exceed 1.0° F., while in table 2, 23 out of 36 (64 percent) of them are

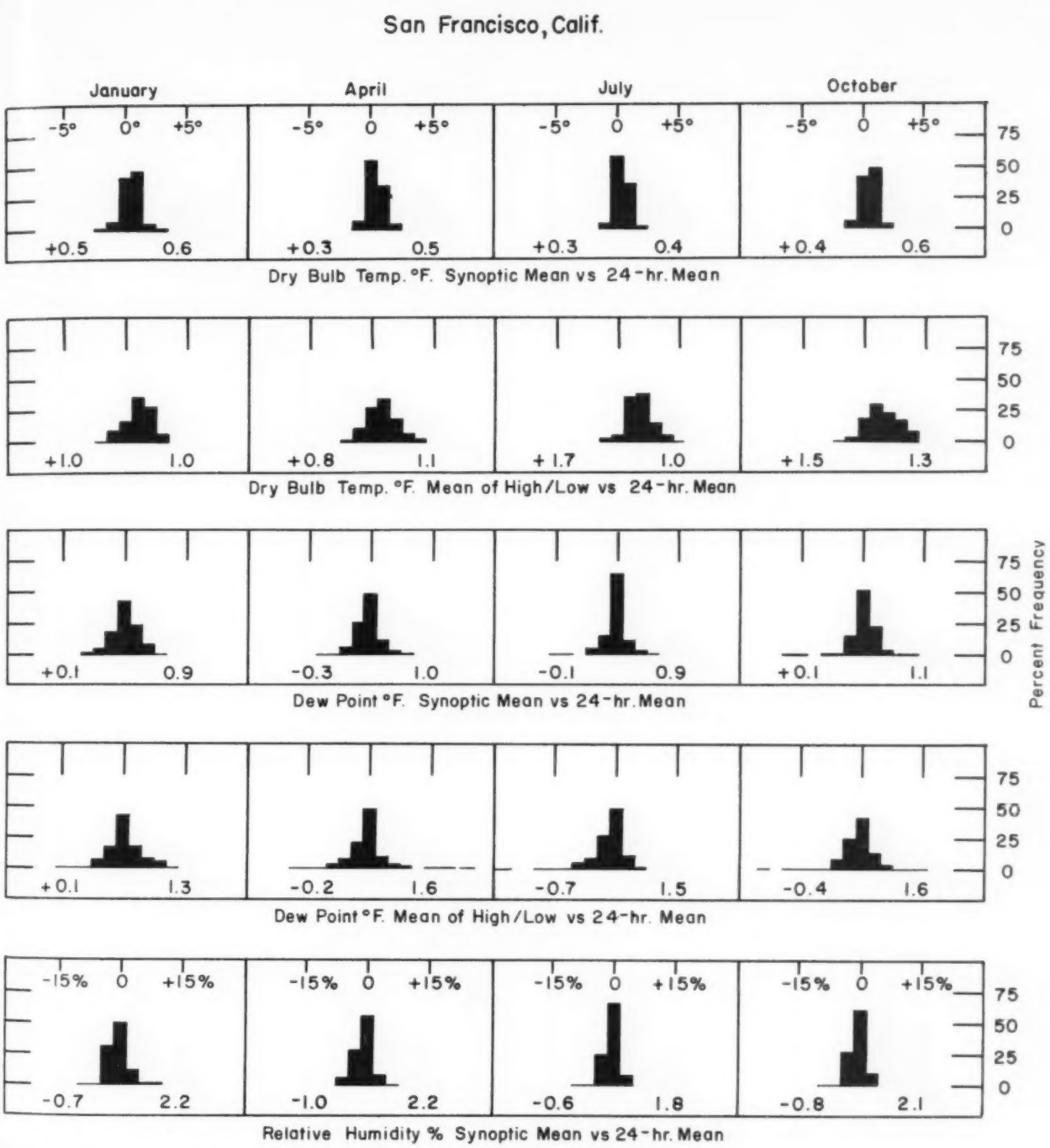

FIGURE 1.—The average of the daily departures from the 24-hour mean, and the frequency distribution and standard deviations of those daily departures for dry bulb temperature, dew point temperature, and relative humidity at San Francisco, Calif. for 5 years of data (1955–59). "Synoptic mean" indicates the daily average of the values recorded at the 4 "synoptic" observations. "Mean of high/low" is the daily average of the highest and lowest hourly values.

larger than unity. None of the standard deviations in table 1 exceeds 1.5° (1.4° in January at Bismarck is the largest) while in table 2 there are 4 cases which exceed 1.5°.

Bigelow [5] used hourly temperature data from 25 stations for an 11-year period (1891–1901) to obtain average corrections to reduce means computed by various combinations to "true" 24-hour means. He plotted these

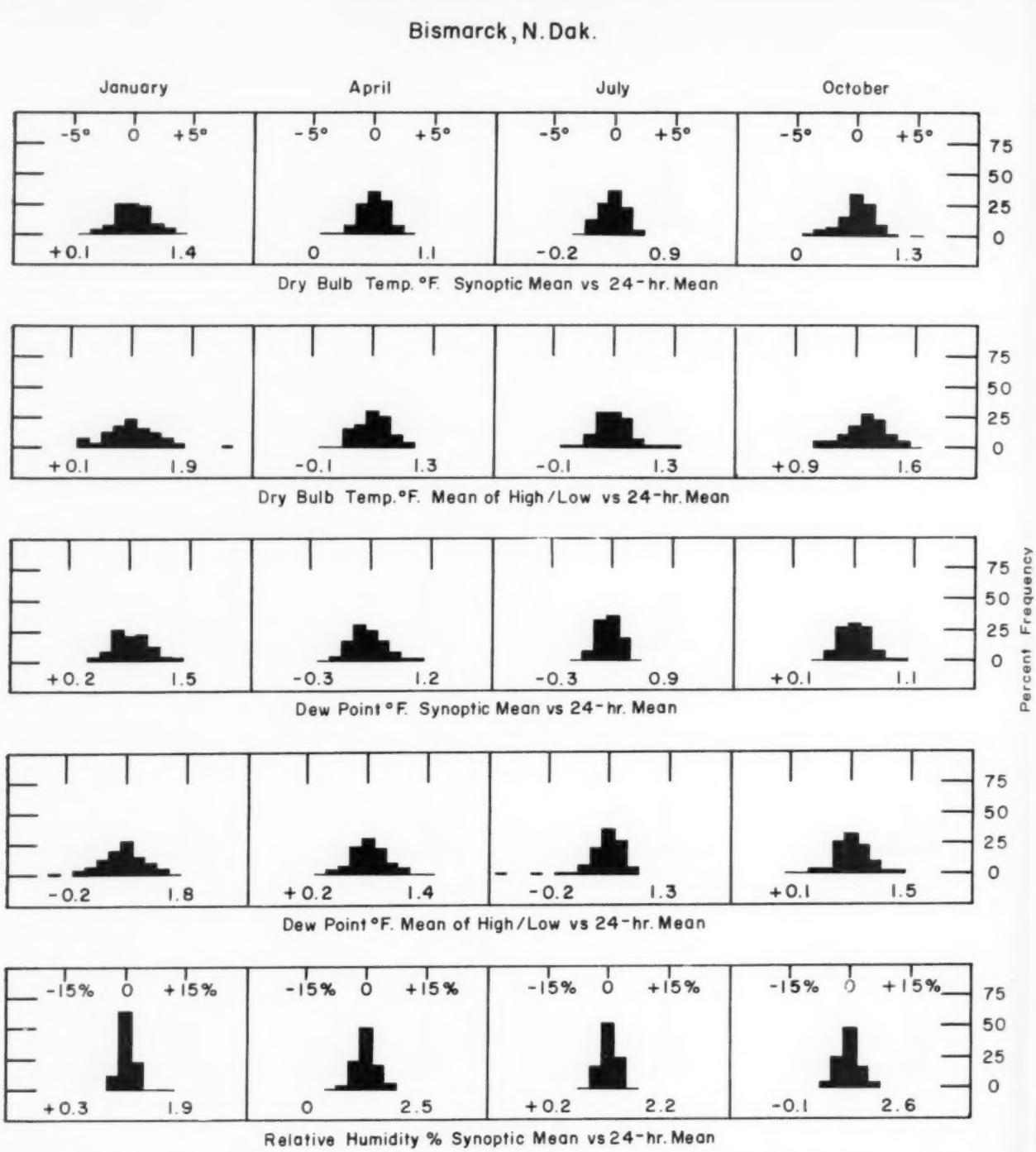

FIGURE 2.—The average of the daily departures from the 24-hour mean, and the frequency distribution and standard deviation of those daily departures for dry bulb temperature, dew point temperature, and relative humidity at Bismarck, N. Dak. for 5 years of data (1955–59).

corrections on maps for each month, drew isolines, and interpolated correction terms for a considerable list of stations. His corrections (with sign reversed to make them comparable to the departures presented in this study) for a list of stations and months comparable to those of this study are given in table 6, column A. Corresponding values from the present study (taken from table 2) are listed for comparison. It was recognized

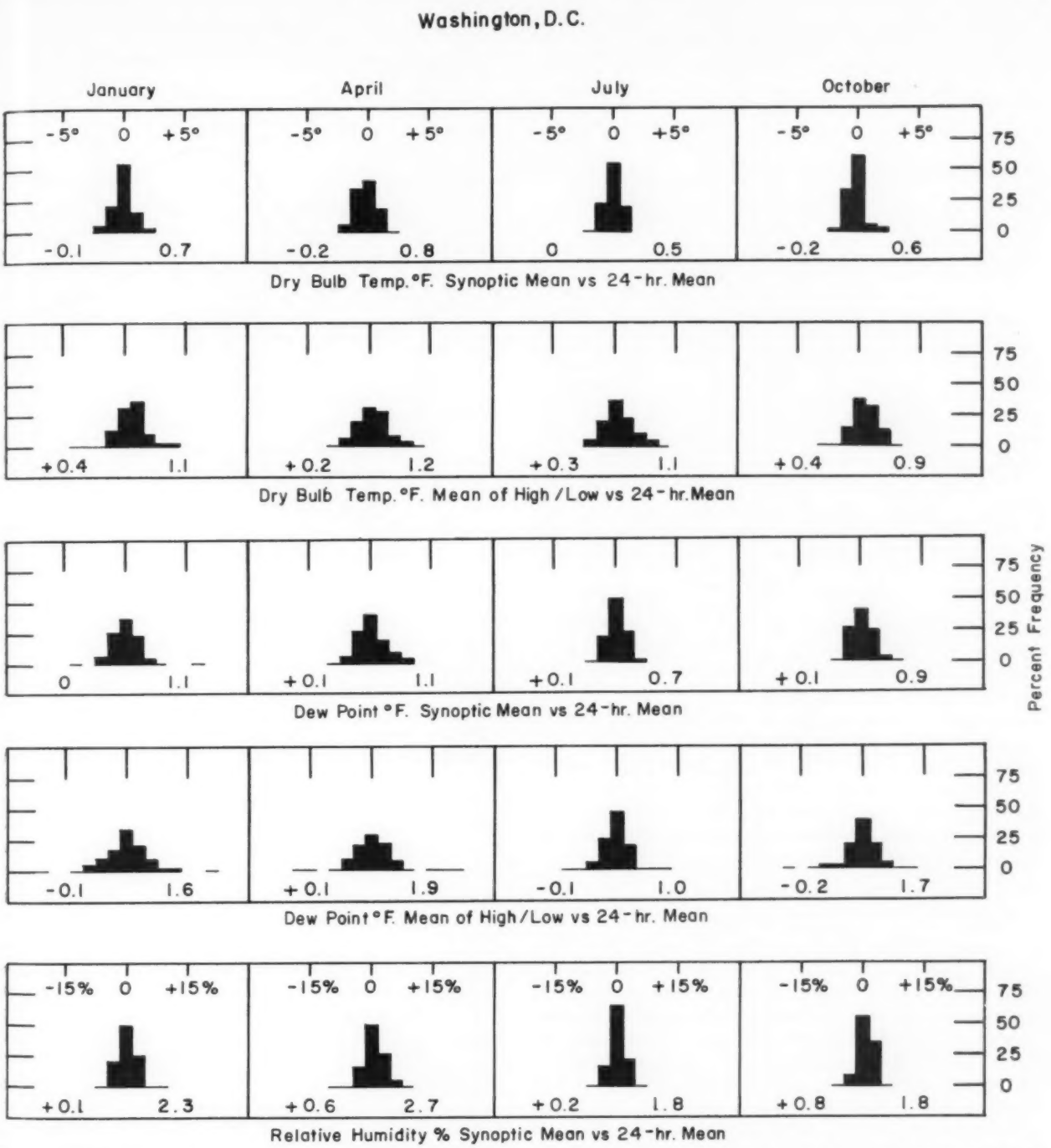

FIGURE 3.—The average of the daily departures from the 24-hour mean, and the frequency distribution and standard deviation of those departures for dry bulb temperature, dew point temperature, and relative humidity at Washington, D.C. for 5 years of data (1955–59).

that changes in station location or other changes during the intervening half-century may have introduced reasons for differences between results of the two studies. However, it was considered that a historical comparison would be of some interest. There is good agreement between the two sets of data in the cases of larger departures. See, for example, San Francisco in April, July, and October. In most other cases the sign and magnitude of the departures are in fair agreement. There are only a few large contradictions, the most obvious being at Salt Lake City in April and October and at Bismarck in January.

TABLE 3.—*Dew point: Synoptic mean vs. 24-hr. mean. Average departure of mean of 4 synoptic observations from 24-hr. mean and the standard deviation of daily departures. 5 years of record, °F.*

Station	January		April		July		October	
	Dep.	S.D.	Dep.	S.D.	Dep.	S.D.	Dep.	S.D.
Seattle	0	0.7	+0.1	0.7	0	0.6	+0.1	0.6
San Francisco	+0.1	0.9	−0.3	1.0	−0.1	0.9	+0.1	1.1
Salt Lake City	+0.2	1.2	−0.3	1.1	−0.3	1.3	−0.1	1.1
Bismarck	+0.2	1.5	−0.3	1.2	−0.3	0.9	+0.1	1.1
Fort Worth	0	1.4	−0.1	1.6	−0.1	0.7	0	1.1
St. Louis	0	1.5	−0.1	1.1	0	0.7	0	1.1
Boston	0	1.1	0	0.9	0	0.6	0	0.9
Washington	0	1.1	+0.1	1.1	+0.1	0.7	+0.1	0.9
Miami	−0.1	0.8	+0.1	0.6	+0.1	0.5	0	0.5

TABLE 4.—*Dew point: Mean of high/low vs. 24-hr. mean. Average departure of mean of highest and lowest hourly from 24-hr. mean and the standard deviation of daily departures. 5 years of record, ° F.*

Station	January		April		July		October	
	Dep.	S.D.	Dep.	S.D.	Dep.	S.D.	Dep.	S.D.
Seattle	−0.3	1.0	−0.5	1.2	−0.2	0.8	−0.2	0.8
San Francisco	+0.1	1.3	−0.2	1.6	−0.7	1.5	−0.4	1.6
Salt Lake City	−0.2	1.4	−0.2	1.3	−0.5	1.5	+0.1	1.0
Bismarck	−0.2	1.8	+0.2	1.4	−0.2	1.3	+0.1	1.5
Fort Worth	0	1.7	+0.1	2.3	−0.4	0.8	−0.3	1.6
St. Louis	−0.1	1.6	0	1.4	−0.1	0.8	−0.1	1.2
Boston	−0.1	2.1	+0.2	1.5	0	1.0	+0.1	1.6
Washington	−0.1	1.6	+0.1	1.9	−0.1	1.0	−0.2	1.7
Miami	−0.3	1.1	−0.5	1.2	−0.3	0.6	−0.2	0.7

A comparison of the average departures and standard deviations of corresponding individual station months between table 1 and table 2 shows that in every case either one or both are larger in table 2 than in table 1. This merely serves to substantiate the work of others regarding the mean of the daily maximum and minimum. The present purpose is not to make a case either for or against one of these methods but rather to determine whether or not daily mean values of dew point and relative humidity by one or the other of these methods are as reliable, by comparison, as are daily mean values of temperature.

DEW POINT TEMPERATURE

Tables 3 and 4 present the averages and the standard deviations of the daily departures of daily mean dew points computed and listed in the same way as were the temperature data in tables 1 and 2. Dew point is generally considered to be a much more conservative element than is dry bulb temperature. This conservatism may be responsible for the generally smaller average departures from the "true" daily mean. In table 3 (mean of four synoptic observations) the greatest monthly average departure is 0.3°, while in table 1 (dry bulb by the same method) there were 2 cases of 0.5° or greater. In table 4 (mean of daily highest and lowest hourly) there are 3 cases of average departure of 0.5° or greater (the largest being 0.7°), while in the corresponding table 2 (for dry bulb temperature) there are 9 cases of average departures of 0.5° or greater with an extreme of 1.7°. In other words, so far as average departure is concerned, each of the two methods (synoptic mean and mean of high and low) has less departure when used for dew point than when used for dry bulb. Also, as in the case of dry bulb, the departures of means obtained from the sum of the daily highest and lowest hourly observations (table 4) tend to be slightly larger than those obtained from the four synoptic observations (table 3).

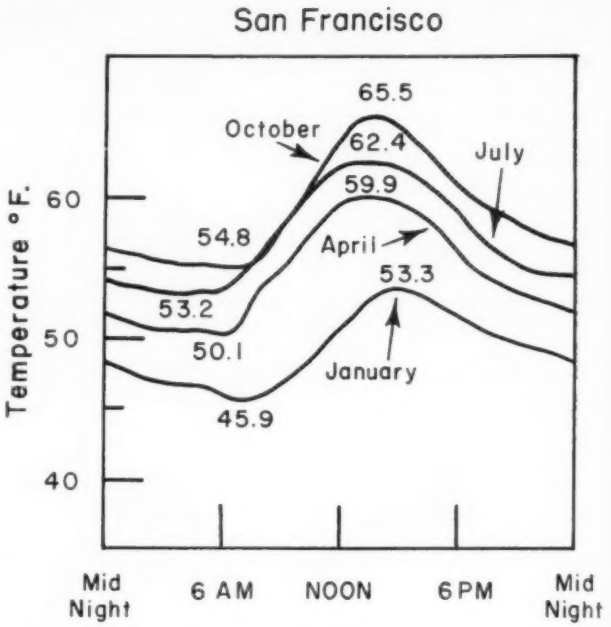

FIGURE 4.—Mean hourly temperature for selected months (1891–1930), San Francisco, Calif.

Before discussing the practical significance of the standard deviations in tables 3 and 4 (compared with those in tables 1 and 2) it is in order to examine the units involved. The reasons for adopting a class interval of 3 percent relative humidity in figures 1, 2, and 3 are discussed in the Appendix. A similar examination of the psychrometric tables was made to determine whether or not, for the purposes of this study, a unit of 1° F. in dry bulb temperature could reasonably be compared to a unit of 1° F. in dew point temperature. It was found that at temperatures near or above freezing, when the corresponding relative humidity is 50 percent or higher, a change of 1° F. in the dry bulb is accompanied by a corresponding change (at a fixed relative humidity) of only slightly more than 1° F. in the dew point. At high temperatures and relative humidities the 1:1 ratio is almost exact. In the vicinity of 60° F. at 50 percent relative humidity the ratio is about 1:1.2. In the range 20° F. to 40° F. at 50 percent relative humidity the ratio averages a little higher, about 1:1.4, and increases rapidly at lower temperatures and lower relative humidities. That is, at lower temperatures and lower relative humidities, a change of 1° F. in the dry bulb is comparable to a change of from 2° F. to several degrees in the dew point temperature. Therefore, for the practical purposes of this present study, the magnitude of the average departures and standard deviations in tables 3 and 4 may be considered generally comparable with

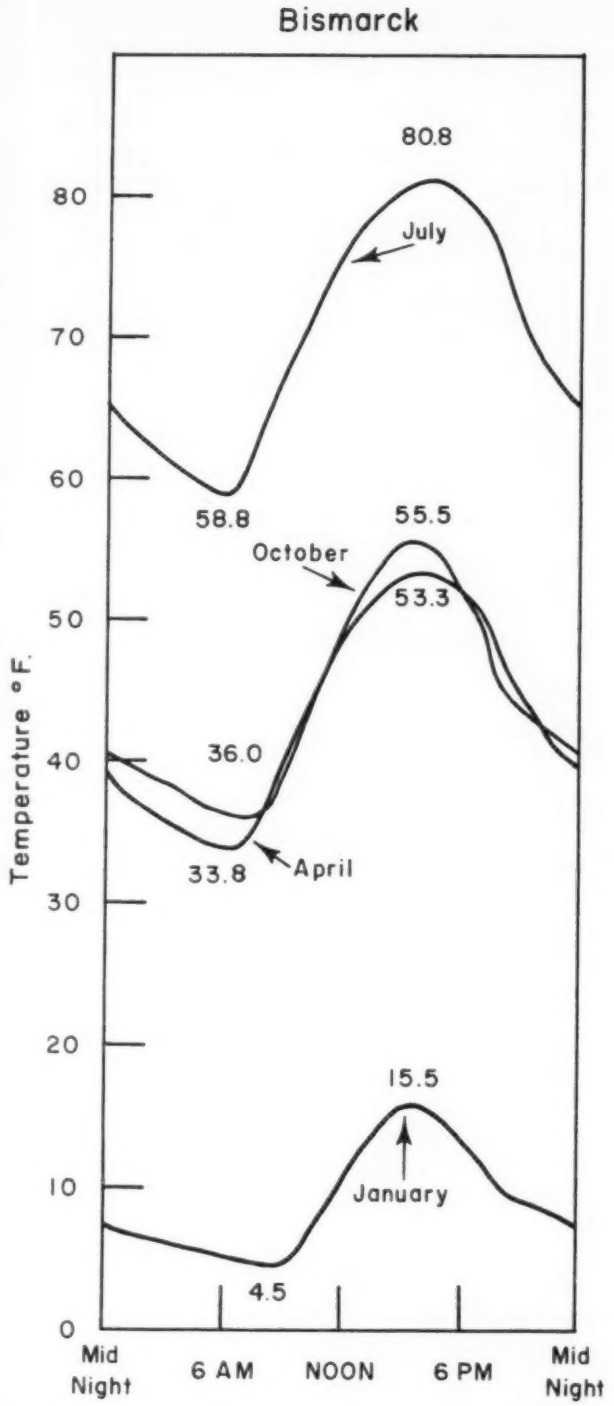

FIGURE 5.—Mean hourly temperature for selected months (1894–1930), Bismarck, N. Dak.

those in tables 1 and 2 except in months with high frequencies of daily mean temperatures near or below about 20° F. or with daily mean relative humidities below 50 percent. In the present study only the January data for

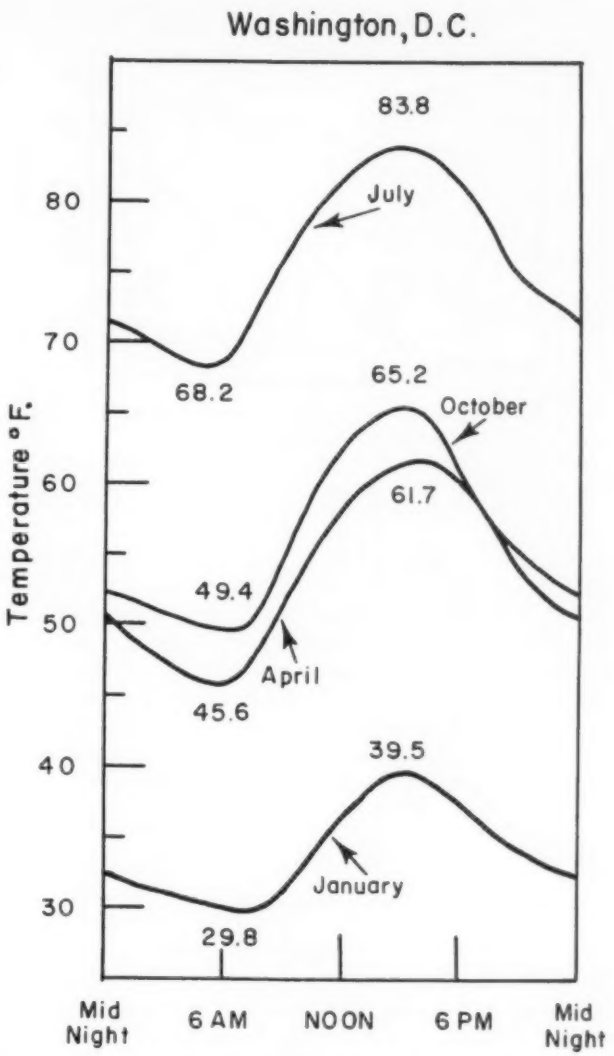

FIGURE 6.—Mean hourly temperature for selected months (1890–1930), Washington, D.C.

Salt Lake City, Bismarck, St. Louis, and Boston would be affected, and these only marginally. The following discussion will proceed on the basis that the comparisons are valid with the exceptions just mentioned.

A comparison of the standard deviations in tables 1 and 3 shows that in January at all stations the standard deviations are larger in the case of dew point (table 3) than in the case of dry bulb (table 1). However, the increases are not large and may be due in part to the effect of low winter temperatures discussed in the preceding paragraph. In April there is a tendency toward only slightly larger standard deviations in table 3, while in July and October there are actually a few decreases in table 3.

A similar comparison between tables 2 and 4 shows very much the same tendency. In January most stations show a small increase, although at Miami the reverse is true with a large decrease (from 2.1 to 1.1) in the standard

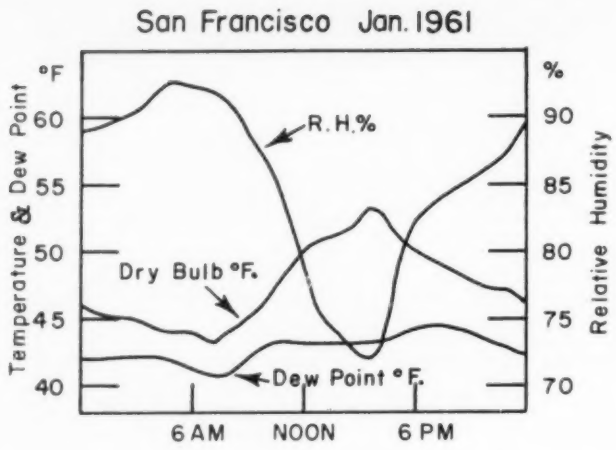

FIGURE 7.—Mean hourly values of temperature, dew point, and relative humidity for January 1961 at San Francisco, Calif.

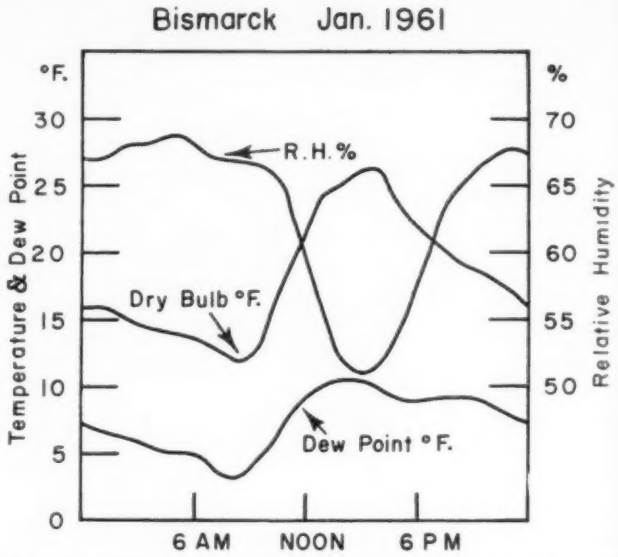

FIGURE 8.—Mean hourly values of temperature, dew point, and relative humidity for January 1961 at Bismarck, N. Dak.

deviation. In April (table 4) the standard deviation at Fort Worth of 2.3° F. is the largest in tables 1, 2, 3, and 4. In July, only two stations show a larger standard deviation in table 4 than in table 2, one shows no change, while six show a smaller value in table 4. In summary, the following numbers of standard deviations in excess of the indicated limits in each of these tables gives some measure of the relative usefulness of these methods when applied to dry bulb and when applied to dew point:

	Standard deviation		
	>1	>1.5	>2
Table 1	10	0	0
Table 3	17	1	0
Table 2	23	4	1
Table 4	26	12	2

Briefly, then, it can be said that average departures are slightly smaller and standard deviations slightly larger in tables 3 and 4 than in tables 1 and 2. The larger standard deviations might be expected in part because of the relationship of temperature and dew point at low temperatures and low relative humidities.

RELATIVE HUMIDITY

Relative humidity is a bilaterally limited element ([4], pp. 43–46). That is, it has both an upper (100 percent) and lower (0 percent) limit. In many climates and seasons the 100 percent upper limit is frequently approached or reached. For these reasons there are no known plans to compute daily means based on daily maximum and minimum values. However, the mean of the four synoptic observations has been used by several workers as an estimate of the daily mean. This present study is limited to a comparison of daily means computed from the 24 hourly values with those computed from the four synoptic observations. The relative significance of a change of 1° F. in dry bulb temperature and a change of 1 percent in relative humidity is discussed in the Appendix; it indicates that as a conservative estimate a

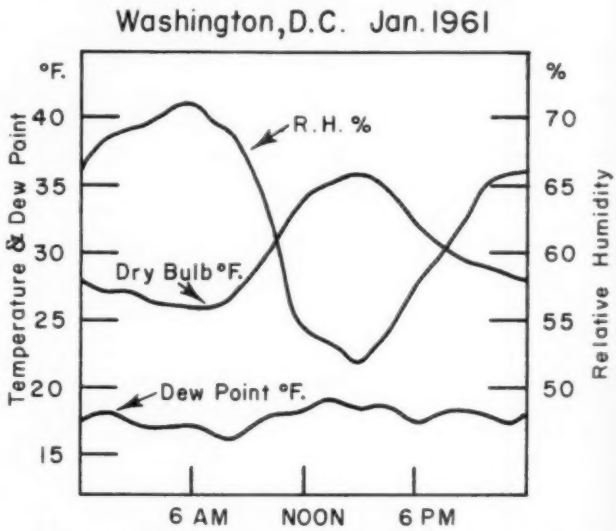

FIGURE 9.—Mean hourly values of temperature, dewpoint, and relative humidity for January 1961 at Washington, D.C.

TABLE 5.—*Relative humidity: Synoptic mean vs. 24-hr. mean. Average departure of mean of 4 synoptic observations from 24-hr. mean and the standard deviation of daily departures. 5 years of record, percent*

Station	January		April		July		October	
	Dep.	S.D.	Dep.	S.D.	Dep.	S.D.	Dep.	S.D.
Seattle	0	2.1	−0.2	2.0	+0.2	1.8	−0.4	1.8
San Francisco	−0.7	2.2	−1.0	2.2	−0.6	1.8	−0.8	2.1
Salt Lake City	−0.2	2.7	−0.5	2.9	+0.5	2.1	−1.3	2.9
Bismarck	+0.3	1.9	0	2.5	+0.2	2.2	−0.1	2.6
Fort Worth	−0.2	2.1	−0.1	3.2	+0.2	1.9	+0.3	2.1
St. Louis	−0.1	2.4	+0.2	2.9	+0.3	1.8	+0.4	2.5
Boston	+0.2	2.0	+0.3	2.3	0	1.8	+0.7	1.7
Washington	+0.1	2.3	+0.6	2.7	+0.2	1.8	+0.8	1.8
Miami	+0.8	1.9	+1.1	1.9	+0.8	1.9	+1.2	1.8

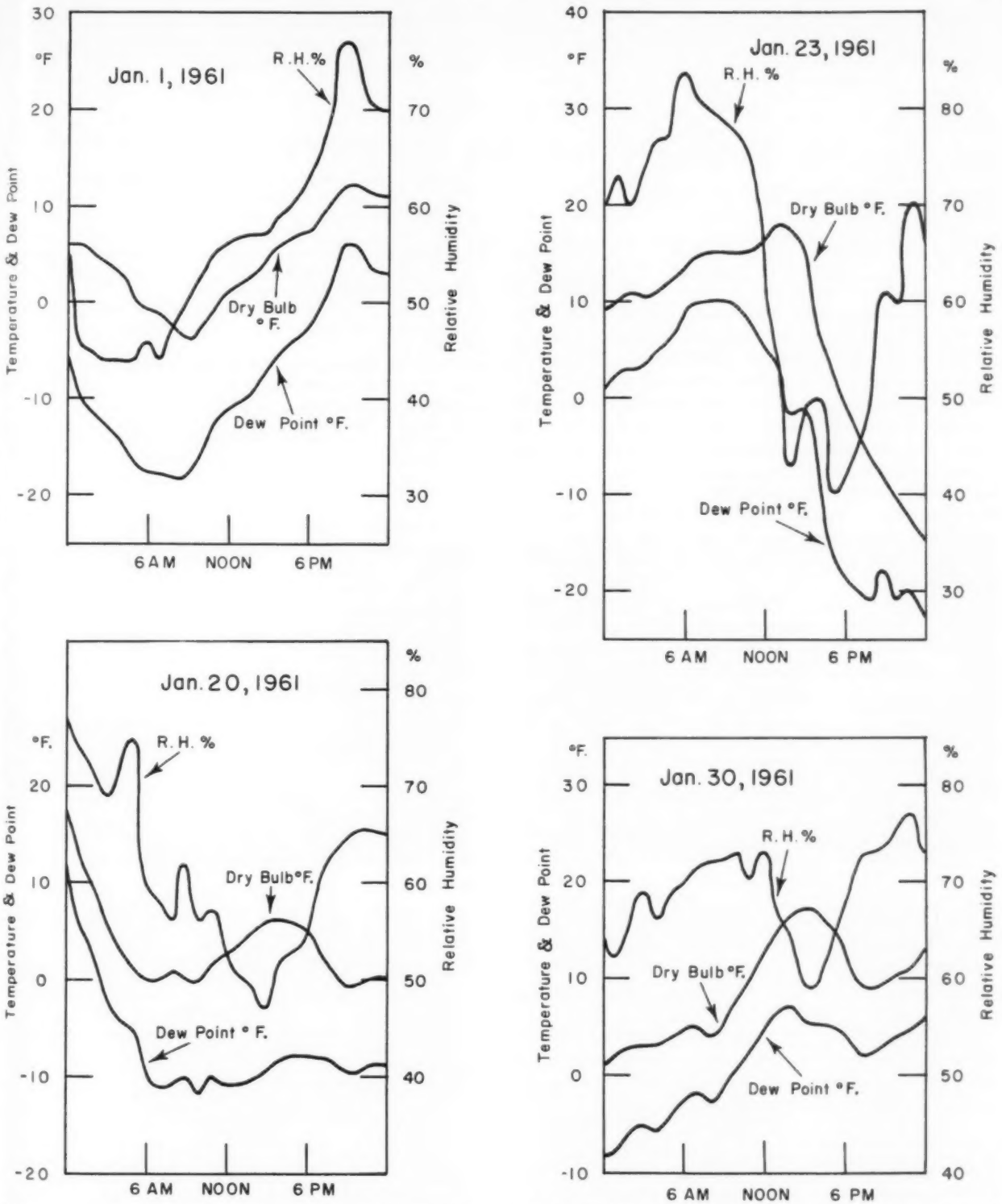

FIGURE 10.—Daily march of dry bulb and dew point temperature and relative humidity for selected dates in January 1961 at Bismarck, N. Dak.

unit of 3 percent relative humidity is comparable, for these purposes, with a unit of 1° F.

Table 5 lists the average departures and standard deviations of daily departures of daily mean relative

TABLE 6.—*Dry bulb temperature (°F.). Average departure of mean of highest and lowest hourly from 24-hr. mean: Column A according to Bigelow [5], and Column B according to this study, table 2.*

Station	January		April		July		October	
	A	B	A	B	A	B	A	B
Seattle	+0.5	+0.1	+0.5	+0.2	+0.5	+0.4	+0.8	+0.3
San Francisco	+0.4	+1.0	+1.0	+0.8	+1.3	+1.7	+1.4	+1.5
Salt Lake City	+0.3	+0.5	−0.5	0	−1.0	−0.9	−0.1	+0.6
Bismarck	−0.5	+0.1	+0.3	−0.1	−0.2	−0.1	+0.7	+0.9
Fort Worth	+0.3	+0.4	+0.3	+0.1	+0.4	+0.2	+0.3	+0.1
St. Louis	+0.2	−0.1	+0.3	+0.1	+0.2	+0.2	+0.5	+0.4
Boston	−0.2	0	+0.5	+0.6	+0.5	+0.4	+0.4	+0.1
Washington	+0.1	+0.4	−0.1	+0.2	+0.5	+0.3	+0.3	+0.4
Key West	+0.2	.....	+0.2	.....	−0.1	.....	0	.....
Miami	.....	+0.1	.....	+0.1	.....	+0.3	.....	+0.4

humidities computed by two methods. The "true" daily mean is the average of the 24 hourly values. The other is the mean of the 4 synoptic observations. The values are expressed in units of percent relative humidity. They should be divided by 3 to be comparable to the dry bulb temperature data in tables 1 and 2. On this basis the largest average departure in table 5 (−1.3 percent at Salt Lake City in October) is appreciably smaller than any in table 1 and falls far short of the largest in table 2 (+1.7 at San Francisco in July). Similarly, in all cases the individual station-month values in table 5 are either smaller than or roughly comparable to their counterparts in tables 1 and 2.

In the case of standard deviations of daily departures, a similar comparison shows very little difference between tables 1 and 5. About two-thirds of the corresponding individual values are larger in table 1 than in table 5 but the differences are small. The largest single value in table 1 is 1.4° F. at Bismarck in January and in table 5 it is 3.2 percent at Fort Worth in April. On a 3 to 1 basis the 3.2 percent is comparable to, but smaller than the 1.4° F.

4. CONCLUSIONS

The purpose of this study was to compare certain methods of computing daily mean values of dew point and relative humidity with similar computations of daily mean dry bulb temperature. The comparisons which were made permit the following generalizations:

1. Daily mean dew point temperatures computed from the four synoptic observations do not vary from the "true" mean any more than daily mean dry bulb temperatures computed in the same way.

2. Daily mean dew point temperatures computed from the daily highest and lowest hourly values do not vary from the "true" mean any more than daily mean dry bulb temperatures computed in the same way.

3. Daily mean dew point temperatures computed from the four synoptic observations vary less from the "true" mean than those computed from the daily highest and lowest hourly values. The difference between the two methods is about the same for dew point as it is for dry bulb temperature.

4. Daily mean relative humidities computed from the four synoptic observations vary less from the "true" mean than daily mean dry bulb temperatures computed from either the four synoptic observations or from the daily maximum and minimum.

REFERENCES

1. M. A. Kohler, T. J. Nordenson, and W. E. Fox, "Evaporation from Pans and Lakes," U.S. Weather Bureau *Research Paper*, No. 38, May 1955, 21 pp.
2. C. H. M. van Bavel and F. J. Verlinden, "Agricultural Drought in North Carolina," *Technical Bulletin* No. 122, North Carolina Agricultural Experiment Station, Raleigh, June 1956.
3. J. E. Newman, R. H. Shaw, and V. E. Suomi, "The Agricultural Weather Station, Its Instruments, Observations, and Site Requirements," *Bulletin* 537, Agricultural Experiment Station, Madison, Wis., June 1959.
4. V. Conrad and L. W. Pollak, *Methods in Climatology*, 2d ed., Harvard University Press, Cambridge, 1950, 459 pp. (pp. 155–164).
5. Frank H. Bigelow, "Report on the Temperatures and Vapor Tensions of the United States," *Bulletin S*, U.S. Weather Bureau, April 1909.
6. J. Murray Mitchell, Jr., "Effect of Changing Observation Time on Mean Temperature," *Bulletin of the American Meteorological Society*, vol. 39, No. 2, Feb. 1958, pp. 83–89.

APPENDIX

The original frequency distribution computations for relative humidity were based on class intervals of one percent. For graphical representation, this interval was too small and gave a very flat distribution which could not be compared with the temperature distribution.

It was decided to consider a larger class interval, one comparable in physical meaning to a temperature unit of 1° F. Relative humidity is of interest in evaporation problems as a means of estimating vapor pressure deficit [1, 2]. Therefore, a unit of relative humidity was sought which would correspond to 1° F. so far as their respective relation to changes in vapor pressure is concerned. The following approximate equivalents were taken from standard psychrometric tables as the amount that the vapor pressure would change with a change of 1° F. temperature or with a change of 1 percent relative humidity.

At this temperature:	*A change of 1° F. corresponds to a change in vapor pressure of:*	*A change of 1 percent relative humidity corresponds to a change in vapor pressure of:*	*Ratio*
20° F.	0.005 inch	0.001 inch	5 to 1
40° F.	0.010 inch	0.0025 inch	4 to 1
60° F.	0.018 inch	0.005 inch	3½ to 1
80° F.	0.033 inch	0.010 inch	3 to 1

From these relationships it was apparent that a class interval for relative humidity in the range of 3, 4, or 5 percent would compare well with a class interval for temperature of 1° F. To make best use of the limited amount of data available, it was decided to use a class interval of 3 percent in these graphs. Following the same line of reasoning, a standard deviation of daily departure of mean relative humidity of 3 percent may be considered to be roughly comparable to a standard deviation of daily departure of mean temperature of 1° F.

Weather Note

SQUALL LINE PASSAGE AT BARROW, ALASKA, JUNE 21, 1960

RONALD J. McCUE, JR.
Weather Bureau Airport Station, Barrow, Alaska
and
G. PHILIP WEEER
Weather Bureau Airport Station, Anchorage, Alaska

[Manuscript received June 19, 1961]

On the evening of June 21, 1960 a squall line, evidenced by a single roll cloud, passed over Barrow, Alaska. Selected photographs of the cloud are reproduced in figure 1. This is an unusual formation at this latitude (71°18′ N.) at any time, but especially unusual for so early in the summer season.

During the afternoon of the 21st the cloud cover over Barrow had increased steadily. The pressure was relatively steady until noon when it began to fall slowly. The temperature began to drop at the same time. By observation time at 2053 AST, Barrow was reporting broken clouds at an estimated 1,500 ft., with an overcast estimated

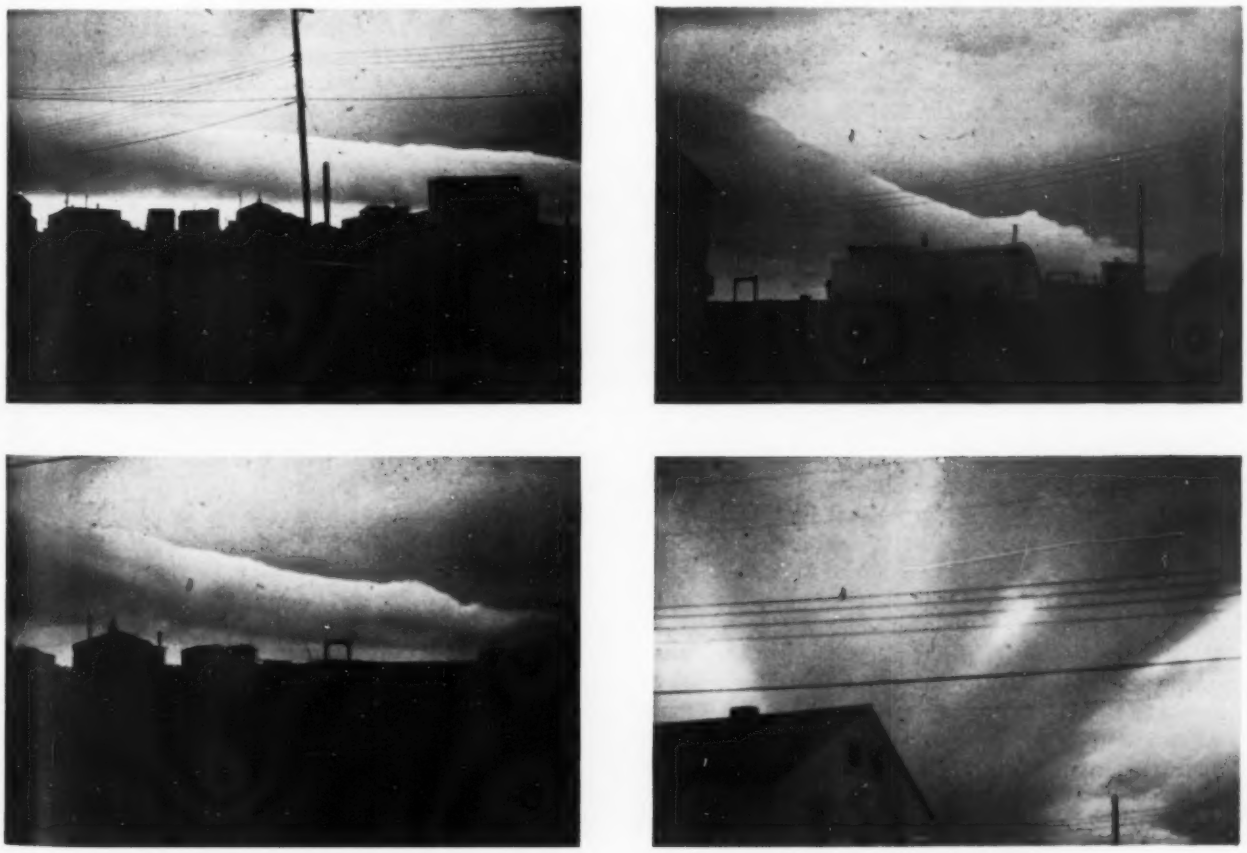

FIGURE 1.—Photographs of the squall line cloud as it passed over Barrow, Alaska, June 21, 1960.

WBAN 10A
Formerly WB Form 1130A also
(Rev. 1-1-55)

U. S. DEPARTMENT OF COMMERCE, WEATHER BUREAU
SURFACE WEATHER OBSERVATIONS

STATION BARROW, ALASKA DATE JUN 21 1960

TYPE 1	TIME (LST) 2	SKY and CEILING (Hundreds of Feet) 3	VISIBILITY (Miles) 4	WEATHER and OBSTRUCTIONS TO VISION 5	SEA LEVEL PRESS. (mbs.) 6	TEMP (°F) 7	DEW PT (°F) 8	WIND DIRECTION 9	WIND SPEED (kts) 10	WIND CHARACTER AND SHIFTS 11	ALTIMETER SET (ins) 12	REMARKS AND SUPPLEMENTAL CODED DATA 13 14A 14B	OBSERVERS INITIALS 15
R	1953	E15 ◐ 80 ◐	15		135	40	37	←↖	8		991	715 1570 48	RM
R	2053	E15 ◐ 80 ⊕	7	RW-	129	38	36	←↖	10		989	RB10	RM
R	2153	E20 ⊕	7	RW--	132	43	39	↖	10		990	SQAL LINE PASSAGE 0720Z	NN
												PRES RISE 0.07	
R	2256	E20 ◐ 40 ⊕	5	RW-	122	43	39	↖	8		987	814 15XX	VL
R	2356	E20 ◐	10		108	43	39	←↖	14		983	RE 41	VL

STATION BARROW, ALASKA DATE JUN 22 1960

TYPE 1	TIME (LST) 2	SKY and CEILING (Hundreds of Feet) 3	VISIBILITY (Miles) 4	WEATHER and OBSTRUCTIONS TO VISION 5	SEA LEVEL PRESS. (mbs.) 6	TEMP (°F) 7	DEW PT (°F) 8	WIND DIRECTION 9	WIND SPEED (kts) 10	WIND CHARACTER AND SHIFTS 11	ALTIMETER SET (ins) 12	REMARKS AND SUPPLEMENTAL CODED DATA 13 14A 14B	OBSERVERS INITIALS 15
R	0056	E20 ◐ 80 ◐	10		108	41	37	↖	10		983		VL
R	0153	E20 ◐ 80 ◐	15+		112	40	38	↑	12+20		984	PRESRR SQAL LINE PASSAGE 1145Z	JNH
												PRES RISE 0.04. NO MARKED WEATHER	
												DEVELOPMENT. 51001 1520 37	
R	0253	E20 ◐ 80 ◐	15+		108	41	37	↑↑	10		983	RADAT 81771066 1137Z	NN

FIGURE 2.—Section of the hourly observations sheet for the period covering the squall line passage.

at 8,000 ft. Visibility was 7 miles in light rain showers, temperature 38° F., wind east-southeast at 10 kt., and pressure 29.890 in.

Just after this observation the roll cloud was seen approaching Barrow from the southwest. Mrs. McCue was the first to notice it and soon the whole community was out watching it pass overhead under the existing overcast. This single roll cloud at about 800 ft. moved across the sky from southwest to northeast. A gust of wind from the southwest accompanied the cloud and wet clothes hanging on the lines flapped up to horizontal positions. Since this was Midsummer Day there was plenty of light at this hour for picture taking.

A pressure rise of 0.07 in. occurred with the squall line passage. By the 2153 observation the low cloud layer had spread to cover 10-tenths of the sky at an estimated 2,000 ft.; visibility was 7 miles with very light showers; temperature 43° F.; wind southeast at 10 kt.; and pressure 29.895 in. Note the 5° jump in temperature in the hour. The hourly observations are reproduced in figure 2.

The synoptic situation on June 21 and 22 in the region of Barrow is illustrated by surface (fig. 3) and 850-mb. (fig. 4) maps. A large low pressure system centered over the Arctic Ocean 600–700 miles west-northwest of Barrow was the controlling circulation feature. The cloud formation was associated with a well-defined trough, oriented from west-northwest to east-southeast, which moved northeastward and northward across northwestern Alaska in the controlling flow around the large low pressure system. The surface trough line, in the vicinity of Kotzebue at 1400 AST, moved northeastward and was approaching Wainwright (located 75 miles southwest of Barrow) at 2000 AST. By 0200 AST, June 22, the trough had passed Barrow and Fletcher's Ice Island T-3 (about 70 miles northwest of Barrow), which reported a thunderstorm and measured 0.31 in. of precipitation during the 6-hour period. The trough was well-defined at 850 mb. also, extending on a northwest-southeast line over St. Lawrence Island at 0200 AST, June 21, and approaching Kotzebue at 1400 AST; the trough was much less well-defined at 0200 AST, June 22.

Only four thunderstorms have been recorded at Barrow in 40 years. The most recent one before the 1960 occurrence was on July 1, 1957.

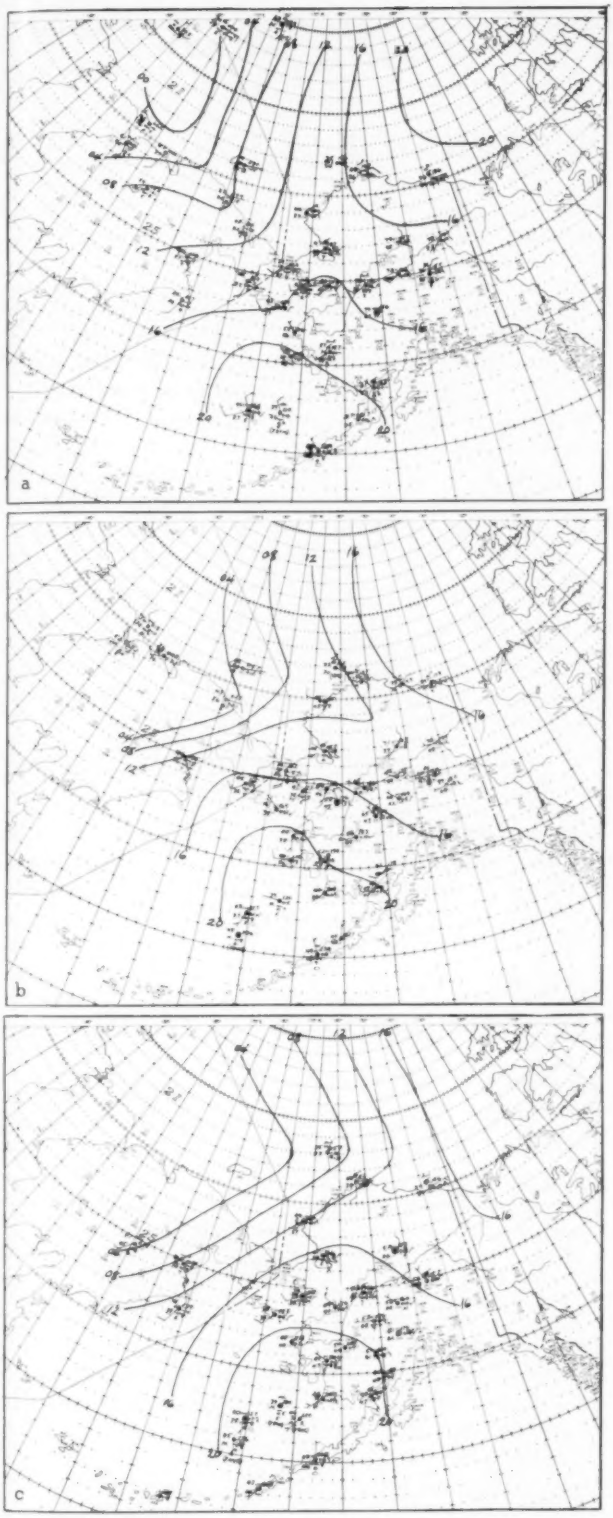

FIGURE 3.—Surface maps for (A) 0000 GMT, (B) 0600 GMT, and (C) 1200 GMT, June 22, 1960. The squall line passage occurred at 0720 GMT, June 22 (2120 AST, June 21).

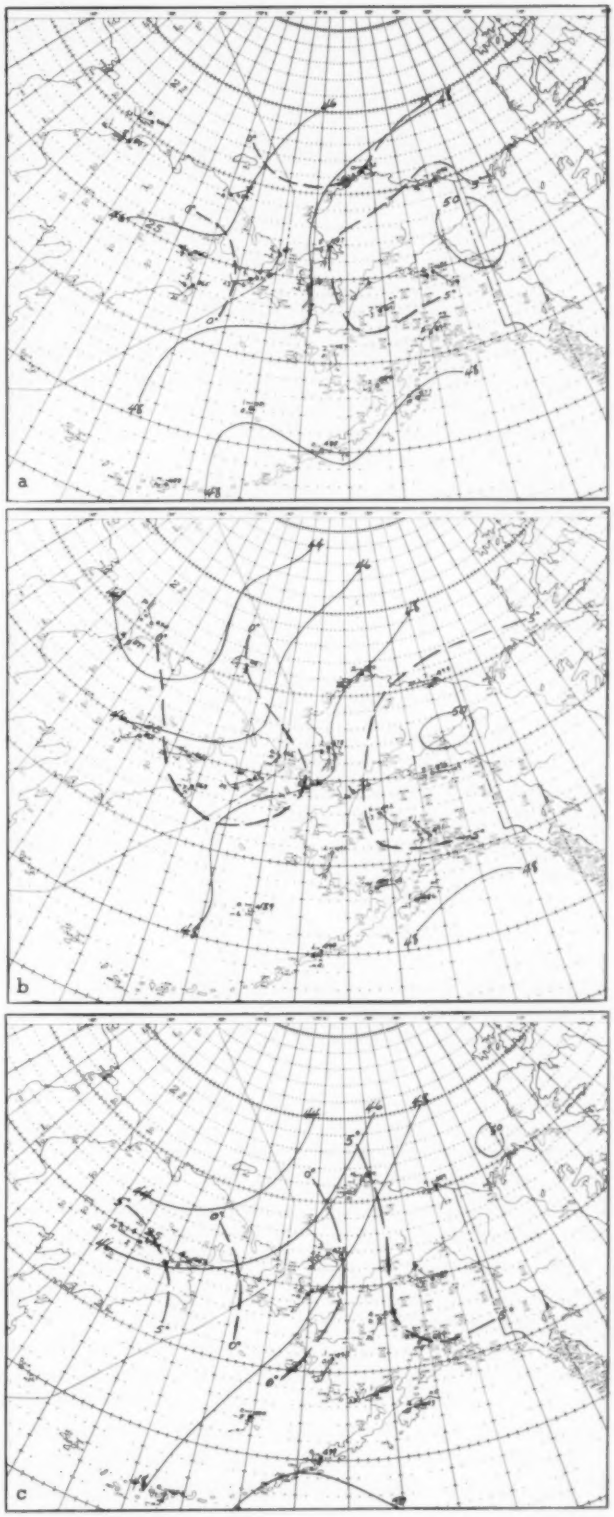

FIGURE 4.—850-mb. maps for (A) 1200 GMT June 21, (B) 0000 GMT, and (C) 1200 GMT June 22, 1960.

THE WEATHER AND CIRCULATION OF JULY 1961

RAYMOND A. GREEN

Extended Forecast Branch, U.S. Weather Bureau, Washington, D.C.

1. INTRODUCTION

July 1961 was the fourth consecutive month in which temperatures averaged cooler than normal in most of the eastern half of the United States (fig. 1). This cool regime began with a sharp temperature reversal from March to April [1], then gradually intensified through June [2], and was finally modified in July. The warming trend in the West, which progressed from initially cool conditions in April to persistent and locally intense heat in June, was reversed in July. Thus the latter month afforded some relief from heat in the West, along with more favorable growing weather for retarded crops in the Corn Belt.

2. MEAN CIRCULATION

The mean 700-mb. circulation for July 1961 (fig. 2) was dominated by blocking and low index conditions, as indicated by the prevalence of positive height anomalies at higher latitudes and negative anomalies at lower latitudes. Blocking was particularly strong in North America and the Pacific, where there were three positive height anomaly centers with departures from normal as much as 200 ft. or more (fig. 2). Also noteworthy was the occurrence of easterly anomalous flow at middle latitudes over much of the Western Hemisphere.

The zonal index, as measured by the net west to east geostrophic flow between latitudes 55° and 35° N. in the western sector of the hemisphere, was 1.1 m.p.s. below normal at both sea level and 700 mb. during July. These are rather large departures for this index during a summer month. It is also of interest that the 5-day mean zonal index routinely computed three times a week, remained continually below normal during the entire month at 700 mb. and during all but one period at sea level. The 700-mb. subtropical westerlies also averaged well below normal (1.3 m.p.s.) for the month as well as during all 5-day periods.

Blocking was related to the displacement of the primary mean 700-mb. jet axis southward from its normal position over much of the hemisphere in July (fig. 3). Greatest displacement was over eastern North America where blocking was strongest. Over northeastern sections of the Atlantic and Pacific northward extension of the subtropical ridges displaced portions of the mean jet northward.

The polar circulation was featured by a deep closed Low surrounded by an almost continuous ring of positive height anomalies (fig. 2). Fast westerlies around this Low were associated with the eastward displacement of most of the normal trough-ridge systems at high latitudes. The ridge normally found near Alaska was flattened and elongated eastward, the Baffin Island Low was shifted eastward to Greenland, and one cell of the Icelandic Low was located in the Norwegian Sea.

Changes of mean 700-mb. height anomaly from June to July (fig. 4) were predominantly positive at high latitudes and negative at low latitudes. Net changes, computed for complete latitude circles at intervals of 5° lat., were strongly positive from 80° to 60° N. and decidedly negative from 50° to 25° N. This indicates an increase in high-latitude blocking from the previous month.

3. CIRCULATION AND TEMPERATURE CHANGES DURING JULY

There were two distinct circulation regimes over and near the North American continent in July. During the first 10 days (represented by the 5-day mean for July 4–8, fig. 5A) an active mean trough retrograded into the eastern United States from the Atlantic, while a well-developed mean ridge dominated the region from Texas northward through central Canada. Temperatures at this time (fig. 5B) were well below normal

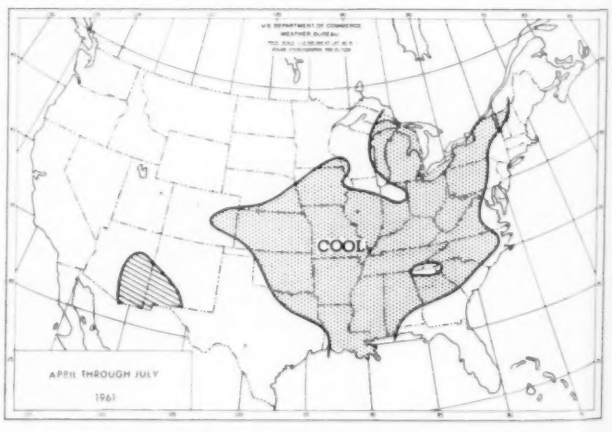

FIGURE 1.—Areas with cooler than normal (stippled) and warmer than normal (hatched) monthly average temperatures for four consecutive months, April through July 1961 (from [5]).

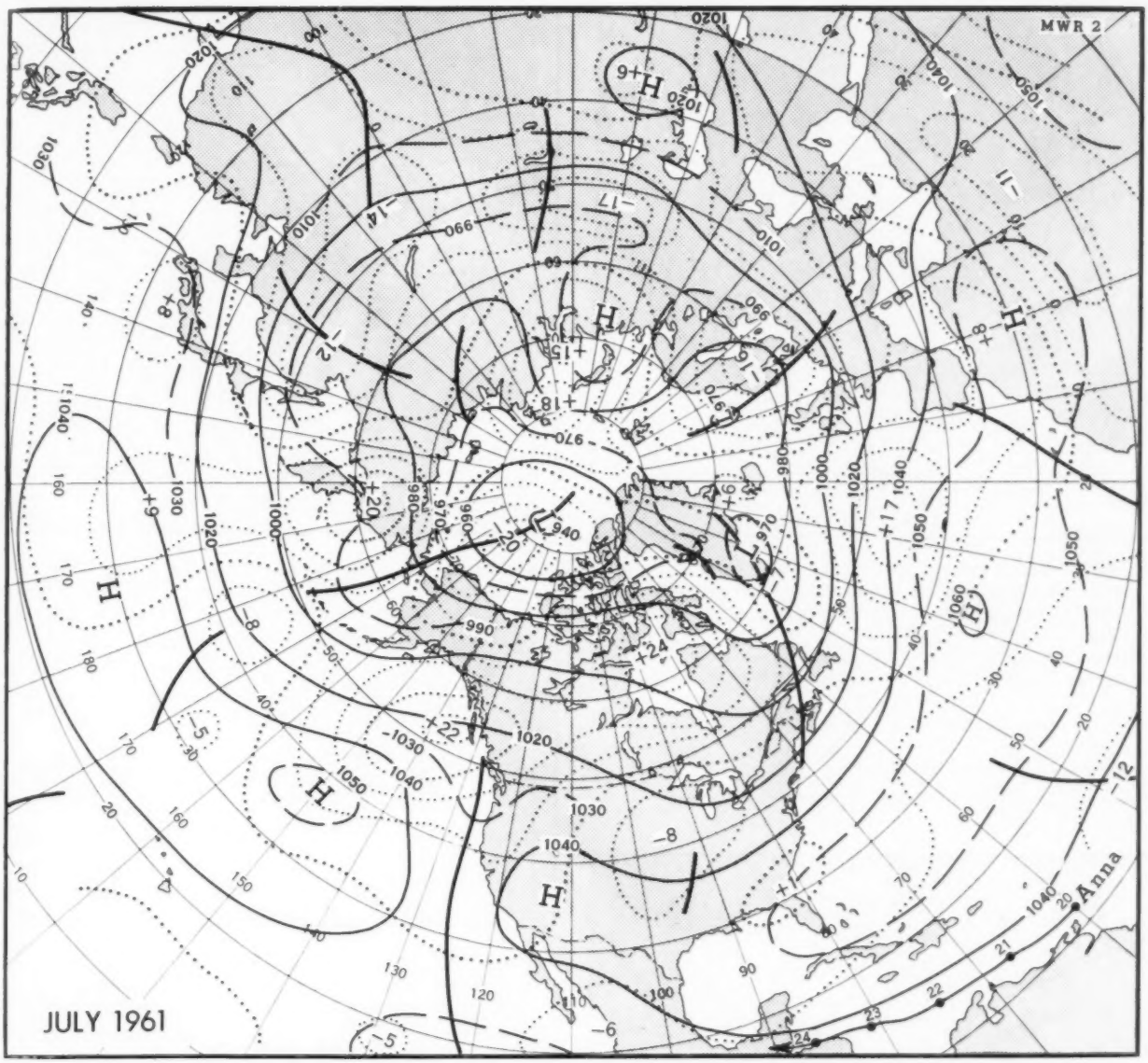

FIGURE 2.— Mean 700-mb. contours (solid with intermediate contours dashed) in tens of feet, and departures from normal (dotted) in 50-ft. intervals for July 1961. High latitude troughs and ridges around the periphery of the deep polar Low were displaced eastward from normal positions. Height anomaly patterns characteristic of blocking were prevalent over much of the hemisphere. Also depicted is the path of hurricane Anna. Large dots and dates indicate 0000 GMT position of storm.

over the eastern half of the country in response to northerly flow from Canada into the vigorous mean trough. Warm temperatures prevailed over the northern Rockies and the northern Plains beneath the mean ridge. Subnormal temperatures in the Southwest were associated with a fairly vigorous mean trough along the west coast, and with the onset of summer showers.

Subsequently, the mean ridge in the eastern Pacific began to grow, a trough developed from the Great Lakes southwestward, and the eastern trough returned rapidly to the Atlantic. The resulting regime (fig. 6A) remained relatively unchanged during the last two-thirds of the month.

During this reversal of circulation the eastern trough was replaced by a ridge and the western ridge by a trough. The parallel reversal of surface temperature produced a remarkable contrast between temperature anomaly patterns of the weeks ending July 9 (fig. 5B) and July 23 (fig. 6B). Weekly average anomalies from the first week to the third warmed as much as 9° F. over the eastern Great Lakes and parts of California and cooled more than 6° F. in the northern Plains.

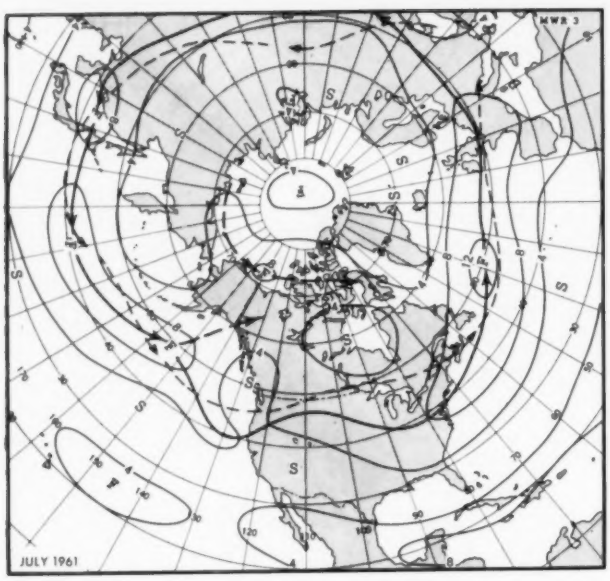

FIGURE 3.—Mean 700-mb. isotachs for July 1961. Heavy solid arrows indicate primary axes of the mean maximum winds; heavy dashed arrows secondary axes; and light dashed arrows, their normal July positions. Primary axes were generally south of normal over the continents but displaced northward by strong subtropical ridges in northeastern sections of both oceans.

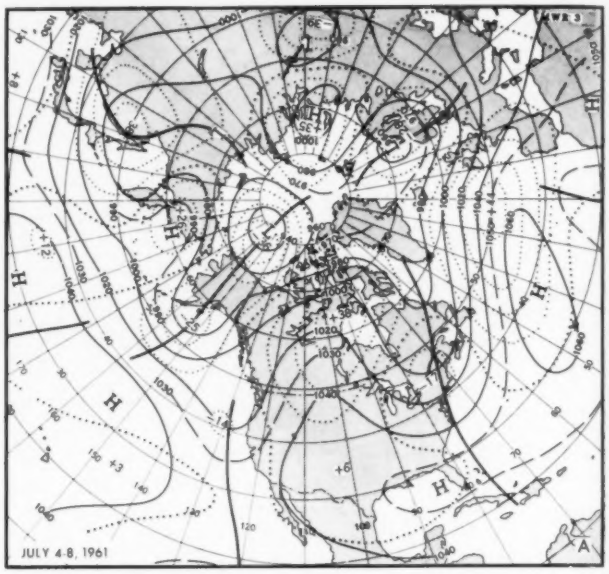

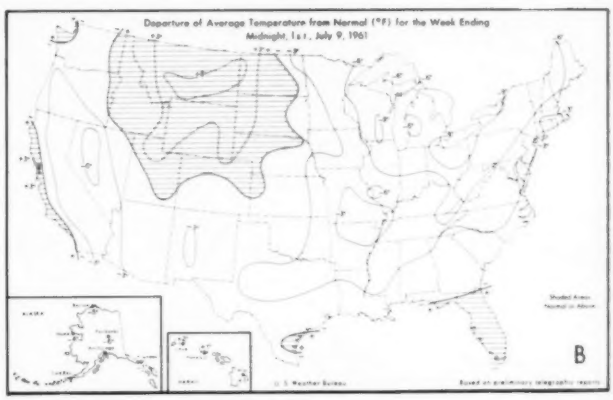

FIGURE 5.—(A) Five-day mean 700-mb. contours and departures from normal (both in tens of feet) for July 4–8, 1961. (B) Departure of average surface temperature (°F.) from normal for the week ending July 9, 1961 (from [5]). These patterns were typical of the first 10 days of the month.

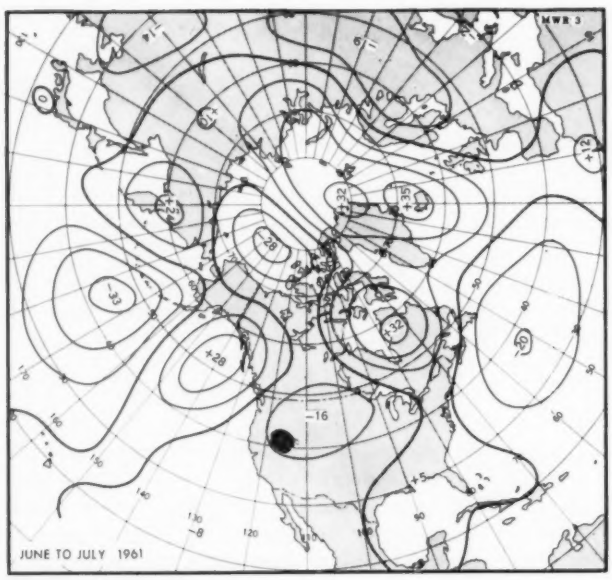

FIGURE 4.—Change in 700-mb. height anomaly (tens of feet) from June to July 1961. Positive changes were predominant at higher latitudes.

4. AVERAGE TEMPERATURE FOR THE MONTH

The contrast of intra-monthly patterns of temperature departure tended to lessen the likelihood for extremes in the monthly pattern (fig. 7). However, new low marks for the monthly average were established at Baton Rouge and Shreveport, La., and at Midland, Tex.

Temperature changes from June to July were closely related to changes in the mean circulation of the mid-troposphere (fig. 4) over North America. Negative changes of 700-mb. height anomaly were generally coincident with cooling over western United States, while positive changes attended warming. There were no changes of month-to-month temperature class from one

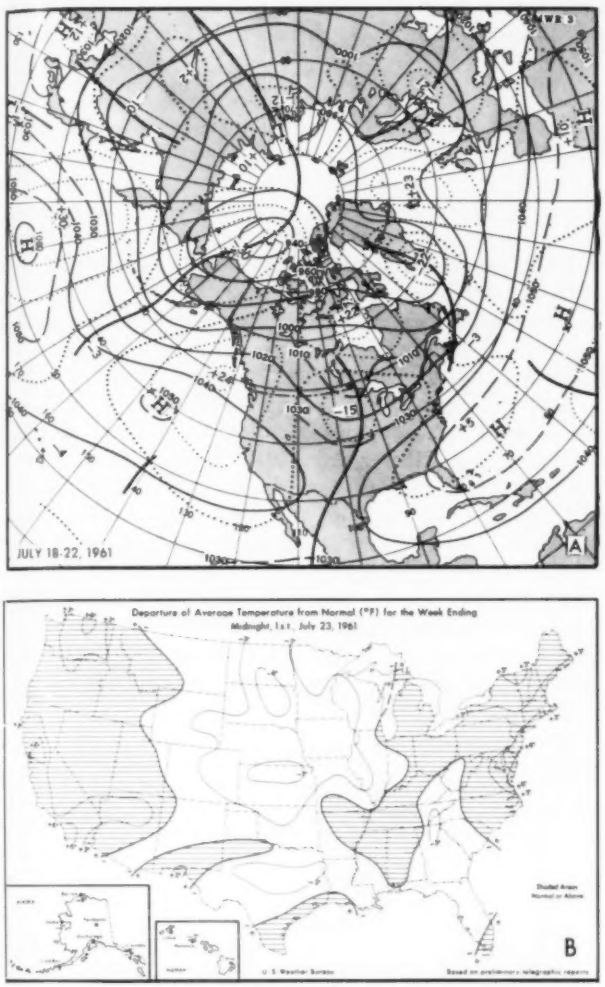

FIGURE 6.—(A) Five-day mean 700-mb. contours and departures from normal (both in tens of feet) for July 18–22, 1961. (B) Departure of average surface temperature (°F.) from normal for the week ending July 23, 1961 (from [5]). These are representative of typical patterns during the last 20 days of the month.

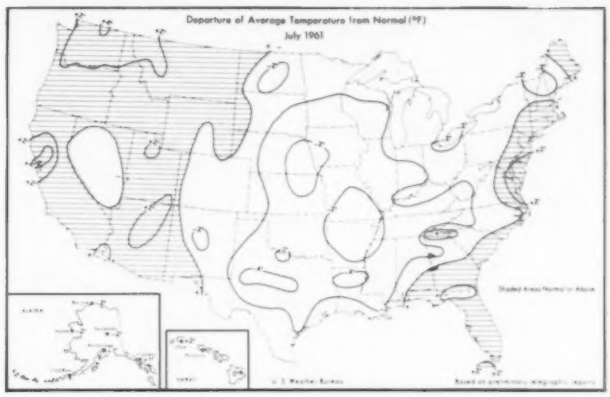

FIGURE 7.—Departure of average temperature from normal (°F.) for July 1961 (from [5]). Greatest departures occurred in Texas and Louisiana (negative) and in California and Washington (positive).

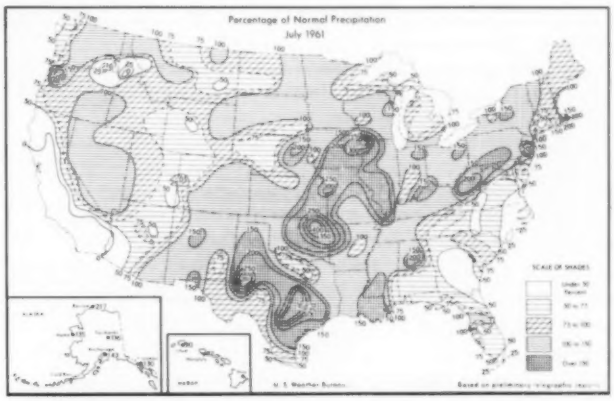

FIGURE 8.—Percentage of normal precipitation for July 1961 (from [5]). Precipitation was especially heavy over much of the southern Plains and the middle Mississippi Valley.

extreme to the other (4-class change). Of 100 representative stations, 72 did not change by more than one class; about the normal degree of persistence for this time of year. Forty-eight stations were cooler while 22 were warmer by one class or more from June to July. The larger number in the cooler category is partly attributable to increased blocking activity from the previous month.

5. PRECIPITATION

Some features of the distribution of precipitation in July (fig. 8) can be explained in relation to the mean circulation. For instance, the belt of abnormal amounts extending from Texas to the Great Lakes was related to the cyclonic vorticity observed in this area, where the normal July circulation is strongly anticyclonic. Although the mean trough in the monthly 700-mb. chart of figure 2 appears weak, its significance is substantiated by the negative height anomalies attending it. Most of this precipitation occurred after the initial circulation regime which ended around the 10th, though large amounts had fallen in southeastern Texas early in the month. Some of the heaviest rain occurred along the zone of maximum frontal activity to the north (fig. 9) Heavy rain associated with frontal activity on the 1st resulted in new records for a 24-hr. amount (6.28 in.) and for July (12.23 in.) at Dubuque, Iowa. A squall line was at least one of the factors leading to development of showers on the 19th which deposited 2.92 in. of rain in an hour and 5.60 in. in 24 hr. at Charleston, W. Va. A new record total for July and any month, 13.54 in. was also established there. Other stations reporting the wettest July were Tulsa, Okla., and Midland, Tex.

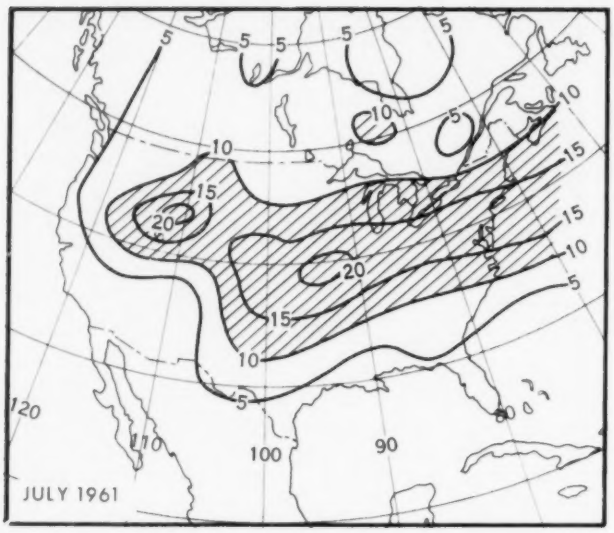

FIGURE 9.—Number of days with fronts in equal-area (66,000 n.mi.²) quadrilaterals for July 1961. The region with 10 or more days with fronts is hatched. Precipitation (fig. 8) exceeded normal in most of the hatched area east of the Continental Divide.

Seasonal rains began in Arizona about on schedule [3] early in the month, ended after a short period, then set in again around the 13th and continued intermittently thereafter. These showers were associated with the injection of moisture from the Gulf of Mexico, induced by normal seasonal evolution of the mean circulation. Nevada and Utah also received appreciable amounts of rain from this source.

Drought continued in the northern Plains, becoming even more severe in some areas. Local showers brought relief in other sections but came too late to do much good. The Southeast was also dry, being under the influence of strong anticyclonic vorticity at both sea level and aloft. Several stations in Florida, including Apalachicola, Lakeland, and West Palm Beach, had record low precipitation totals for the month. Deficits from normal July amounts ranged from 3 to more than 6 inches along the Atlantic coast from Georgia to southern Virginia.

6. TROPICAL STORMS

Hurricane Anna developed southeast of the Windward Islands on the 19th in an easterly wave (see track, fig. 2). Its path and rate of travel were remarkably similar to those of hurricane Abby in July 1960 [4]. Anna moved from the vicinity of the Windward Islands to Central America in approximately 4 days along a track just south of the 10,400-ft. contour (fig. 2).

Four storms were reported in the eastern Pacific, southwestward from central Mexico. Two of them reached hurricane intensity.

In the western Pacific there were five storms, of which three developed into typhoons. One of these traveled northward into Korea from the central section of the Philippine Sea, another hovered around the southern tip of Formosa, and the third dissipated in the East China Sea after a rather long northwestward trajectory from its origin near Iwo Jima.

One of the two storms which failed to develop to typhoon intensity originated east of Luzon, traversed that island, then moved westward into the Chinese mainland. The other traversed a short path which was confined entirely to the East China Sea.

REFERENCES

1. J. F. O'Connor, "The Weather and Circulation of April 1961—Persistent Blocking in Eastern Canada and Cool Weather in the United States," *Monthly Weather Review*, vol. 89, No. 7, July 1961, pp. 256–262.
2. L. P. Stark, "The Weather and Circulation of June 1961—A Hot, Dry Month in the West," *Monthly Weather Review*, vol. 89, No. 9, Sept. 1961, pp. 368–373.
3. R. A. Bryson and W. P. Lowry, "Synoptic Climatology of the Arizona Summer Precipitation Singularity," *Bulletin of the American Meteorological Society*, vol. 36, No. 7, Sept. 1955, pp. 329–339.
4. R. A. Green, "The Weather and Circulation of July 1960—Persistent Heat in the Pacific Northwest," *Monthly Weather Review*, vol. 88, No. 7, July 1960. pp. 257–262.
5. U.S. Weather Bureau, *Weekly Weather and Crop Bulletin, National Summary*, vol. XLVIII, Nos. 18, 23, 27, 28, 30 and 32 May 1, June 5, July 3, 10, 24. Aug. 7, 1961.

U. S. GOVERNMENT PRINTING OFFICE: 1961